

Primordial Black Hole versus Inflaton: Two Chief Systems of the World

Md Riajul Haque^{a,*}, Essodjolo Kpatcha^{b,c,†}, Debaprasad Maity^{d,‡} and Yann Mambrini^{b,§}

^a *Centre for Strings, Gravitation, and Cosmology, Department of Physics,
Indian Institute of Technology Madras, Chennai 600036, India*

^b *Université Paris-Saclay, CNRS/IN2P3, IJCLab, 91405 Orsay, France*

^c *Departamento de Física Teórica, Universidad Autónoma de Madrid (UAM),
Campus de Cantoblanco, 28049 Madrid, Spain and*

^d *Department of Physics, Indian Institute of Technology Guwahati, Guwahati, Assam, India*

We compare the dark matter(DM) production processes and its parameters space in the background of reheating obtained from two chief systems in the early Universe: the inflaton ϕ and the primordial black holes (PBHs). We concentrated on the mechanism where DMs are universally produced only from the PBH decay and the generation of the standard model plasma from both inflaton and PBHs. Whereas the distribution of Primordial Black Holes behaves like dust, the inflaton phenomenology depends strongly on its equation of state after the inflationary phase, which in turn is conditioned by the nature of the potential $V(\phi)$. Depending upon the initial mass and population of PBHs, a large range of DM mass is shown to be viable if reheating is controlled by PBHs itself. Inflaton-dominated reheating is observed to further widen such possibilities depending on the initial population of black holes and its mass as well as the coupling of the inflaton to the standard model sector.

CONTENTS

I. Introduction	1
II. Particle productions through PBH	2
A. Generalities	2
B. Particle production	3
C. Relic abundance	3
D. PBH reheating	4
1. $\beta > \beta_c$	4
2. $\beta < \beta_c$	5
E. Inflaton reheating	8
1. $a_{\text{ev}} < a_{\text{RH}}$	8
2. $a_{\text{ev}} > a_{\text{RH}}$	8
III. Refinements	10
A. The case for extended mass distribution	10
B. Limit on the DM mass from warm dark matter (WDM) constraints	11
1. Generalities	11
2. $\beta > \beta_c$	11
3. $\beta < \beta_c$ (PBH reheating)	12
4. $\beta < \beta_c$ (Inflaton reheating)	12
C. PBH evaporation: Comparison with the exact greybody factor	13
IV. Conclusion	13

Acknowledgments

A. Expression for the critical coupling y_ϕ^c	15
B. Expression for y_ϕ^{th}	16
References	16

I. INTRODUCTION

In 1974, Hawking's proposition that black holes emit radiation was one of the most important results of the last century [1, 2]. It unified thermodynamics, quantum field theory, and general relativity. Only primordial black holes (PBHs), formed in the first instant of the Universe can emit radiation sufficiently important to have some observable effects. On the other hand, the early Universe is also supposed to be populated by a homogeneous field ϕ called inflaton [3–7]. Its decay can also fuel the radiation bath through a mechanism called reheating [8]. The reheating can be non-perturbative in a process called preheating [9–12] or perturbative [13–15]. In any case, at the very end of inflation, the energy density stored in the inflaton is of the order $\rho_{\text{end}}^{\frac{1}{4}} \simeq 10^{15}$ GeV. Such energy corresponds to the horizon mass of the order of 1 gram, where PBHs could have been formed.

Such light black holes have a very short lifetime and can subsequently reheat the Universe, entering in competition with the inflaton. Indeed, recently, it has been shown that the PBHs are capable of reheating the Universe without the need to dominate its energy budget [16]. The main reason for this phenomenon lies in the inflaton equation of state after inflation, which is related

* riaj.0009@gmail.com

† kpatcha@ijclab.in2p3.fr

‡ debu@iitg.ac.in

§ yann.mambrini@ijclab.in2p3.fr

to the behavior of the inflationary potential at the minima. Whereas PBHs behave like dust with a density $\rho_{\text{BH}} \propto a^{-3}$ (a being the scale factor), the inflaton ϕ redshifts faster for inflation equation of state $w_\phi > 0$, as $\rho_\phi \propto a^{-3(1+w_\phi)}$ where w_ϕ is defined by the equation of state $P_\phi = w_\phi \rho_\phi$. Moreover, the PBH decay width¹ $\Gamma_{\text{BH}} \sim M_{\text{P}}^4/M_{\text{BH}}^3$ increases with time as their mass M_{BH} decreases due to evaporation whereas Γ_ϕ decreases with time as the condensate transfers its energy to the plasma. For instance, in the case of a Yukawa type coupling $y_\phi \phi \bar{f} f$ between the inflaton and the Standard

Model (SM), $\Gamma_\phi \propto \rho_\phi^{\frac{2w_\phi}{1+w_\phi}}$ [13, 14]. In other words, the inflaton decay is more efficient *at the beginning* of the reheating process, whereas the PBHs are more efficient *at the end* of their lifetime [16]. These two characteristics, a more diluted and less efficient inflaton with time, help to understand the possibility for the PBH to control the evolution of the temperature in the early Universe. One important point is to note that if $w_\phi > 0.60$, that means for a reheating scenario with a very steep inflaton potential, the BBN bounds of the primordial gravitational wave provide a restriction on the lower limit of the reheating temperature [17, 18].

In the meantime, since the earlier work of Fritz Zwicky [19], the presence of dark matter (DM) has been confirmed at several scales but still not discovered. The recent limits coming from direct detection experiments and the lack of galactic or intergalactic signals put severe pressure on the conventional WIMP paradigm [20]. The scenario where WIMP is produced during the reheating has recently been shown to relax such pressure and allow large parameter regions that can be explored in the near future [21]. Constrained by the direct detection in the conventional scenario, it is imperative to look for some alternative mechanism, particularly for the DM being coupled extremely weakly with the Standard Model. One possibility is feeble interactions with the SM. FIMP candidates [22] can be obtained by the exchange of heavy mediators [23, 24] or gravitons [25–28]. However, there exists the possibility that DM is produced even before the existence of the thermal plasma. Indeed, two energy sources are present at the very end of inflation: inflaton and PBHs, because unstable, are perfect candidates to populate the dark sector. If they both can reheat the Universe, it seems natural to wonder if they can also populate the dark sector. Indeed, they have in common that the inflaton is not charged under the Standard Model, and the PBHs have only gravitational interaction; they should not distinguish the production of a thermal bath and the decay into DM. Note that the same argument can be used to solve the problem of leptogenesis from PBHs and has been recently nicely addressed in [29].

One should then address the issue that the presence of PBHs in an inflaton background would not overproduce the DM. To avoid an overclosure of the Universe, we expect to have constraints on the PBH parameters, namely the fraction $\beta = \frac{\rho_{\text{BH}}}{\rho_\phi}|_{\text{formation}}$ (ratio between the PBH energy density over inflaton energy density at the point of formation) and the formation mass M_{in} of the PBHs formed during the reheating period. Indeed, whereas β determined the density of PBHs in the Universe, M_{in} gives the lifetime of these PBHs to be compared with the inflaton decay rate. For a given DM mass m_j , a larger BH mass M_{in} ensures a smaller width Γ_{BH} , which in turn can avoid overproduction. On the other hand, for a given M_{in} , a DM mass larger than the initial black hole temperature $T_{\text{BH}}^{\text{in}}$ can sufficiently suppress the production rate until the time $T_{\text{BH}} \gtrsim m_j$ also to avoid the overproduction.

Combining these properties of the PBHs with the richness of the inflaton phenomenology opens a large window of parameter space, which was closed without considering the presence of PBHs. We expect the two systems of the world, inflaton, and PBH, to be highly intertwined when calculating the relic density associated with the reheating process. This is exactly the issue we want to address in this paper, organized as follows. After a brief reminder of the reheating mechanism in the presence of PBH, we compute the relic abundance of DM in different scenarios in section II, where we solve and analyze the set of Friedmann equations. In section III, we look into the case of extended mass function and the limit on the DM mass if one considers the constraints from the warm dark matter. We then discuss the influence of exact greybody factors before concluding in section IV.

II. PARTICLE PRODUCTIONS THROUGH PBH

A. Generalities

Being interested in the production of dark matter particles from the evaporation of PBH, we propose first to summarize the main results, which will be useful for our analysis. Even if one can find them in the literature, it is somewhat convenient here to gather the more important equations as they are quite dispersed, see [30–33] for instance. We particularly want to drive the attention of the reader to the specific references [34], [35] and [36], which contain elaborate discussions on the PBH evolution in the early Universe. We also want to add the reference of B. Carr himself [37] which comes back to the historical aspects of the discovery of PBH's evolution. Note that none of these references work in a classical background dominated by the inflaton field, so we had to adapt the results to our specific environment. To compute the relic abundance while *at the same time* ensuring a reheating through the combined inflaton-PBH sources, one has to

¹ throughout our work, we will consider $M_{\text{P}} = 1/\sqrt{8\pi G} \simeq 2.435 \times 10^{18}$ GeV as the reduced Planck mass.

solve the set of Friedmann and Boltzmann equations

$$\begin{aligned}
\frac{d\rho_\phi}{da} + 3(1+w_\phi)\frac{\rho_\phi}{a} &= -\frac{\Gamma_\phi}{H}(1+w_\phi)\frac{\rho_\phi}{a} \\
\frac{d\rho_R}{da} + 4\frac{\rho_R}{a} &= -\frac{\rho_{\text{BH}}}{M_{\text{BH}}}\frac{dM_{\text{BH}}}{da} + \frac{\Gamma_\phi\rho_\phi(1+w_\phi)}{aH} \quad (1) \\
\frac{d\rho_{\text{BH}}}{da} + 3\frac{\rho_{\text{BH}}}{a} &= \frac{\rho_{\text{BH}}}{M_{\text{BH}}}\frac{dM_{\text{BH}}}{da} \\
\frac{dn_{\text{S}}^{\text{BH}}}{da} + 3\frac{n_{\text{S}}^{\text{BH}}}{a} &= \Gamma_{\text{BH}\rightarrow j}\frac{\rho_{\text{BH}}}{M_{\text{BH}}}\frac{1}{aH} \\
\frac{dM_{\text{BH}}}{da} &= -\epsilon\frac{M_{\text{P}}^4}{M_{\text{BH}}^2}\frac{1}{aH}, \quad (2)
\end{aligned}$$

where $\Gamma_{\text{BH}\rightarrow j}$ is the BH decay width associated with dark matter particles and $\epsilon = \frac{27g_*(T_{\text{BH}})\pi}{4 \cdot 480}$ to the *geometric – optics* limit [30]. $g_*(T_{\text{BH}})$ is the number of degrees of freedom at T_{BH} (106.75 for the Standard Model). ρ_R is the radiation energy density whereas n_S is the number density of the dark species S that we will suppose scalar throughout our study.

Solving Eq.(2) gives

$$M_{\text{BH}} = M_{\text{in}}(1 - \Gamma_{\text{BH}}(t - t_{\text{in}}))^{\frac{1}{3}} \quad (3)$$

where t_{in} is the time of formation of the PBH of initial mass M_{in} , and

$$\Gamma_{\text{BH}} = 3 \times \frac{27}{4} \times \frac{g_*(T_{\text{BH}})\pi}{480} \frac{M_{\text{P}}^4}{M_{\text{in}}^3} = 3\epsilon\frac{M_{\text{P}}^4}{M_{\text{in}}^3} \quad (4)$$

its width. M_{in} is defined by

$$M_{\text{in}} = \frac{4}{3}\pi\gamma H_{\text{in}}^{-3}\rho_\phi(a_{\text{in}}) = 4\pi\gamma M_{\text{P}}^2 H_{\text{in}}^{-1}, \quad (5)$$

or where $\gamma = w_\phi^{3/2}$ parameterizes the efficiency of the collapse to form PBHs [38].

B. Particle production

The production rate of any particular species from a BH depends on its intrinsic properties, namely mass and spin. For simplicity, we will consider the spin-zero Schwarzschild BH throughout. The emission rate of a particle of species j with internal degrees of freedom g_j and mass m_j escaping the Schwarzschild horizon of radius R_S per unit of time and energy interval is expressed as,

$$\frac{d^2N_j}{dt dE} = \frac{27}{4}\pi R_S^2 \times \frac{g_j}{2\pi^2} \frac{E^2}{e^{\frac{E}{T_{\text{BH}}}} \pm 1}$$

with $R_S = \frac{M_{\text{BH}}}{4\pi M_{\text{P}}^2}$ and

$$T_{\text{BH}} = \frac{M_{\text{P}}^2}{M_{\text{BH}}} \simeq 10^{13} \left(\frac{1\text{g}}{M_{\text{in}}} \right) \text{ GeV}, \quad (6)$$

which implies

$$\frac{dN_j}{dt} = \frac{27}{4} \frac{g_j \zeta(3)}{16\pi^3} \frac{M_{\text{P}}^2}{M_{\text{BH}}(t)}. \quad (7)$$

Depending upon the PBH masses, we then have two distinct cases. If $m_j \lesssim T_{\text{BH}}^{\text{in}}$, which is the BH temperature at its formation time, we can consider that the production is effective throughout the entire lifetime of the PBH under consideration. Integrating Eq.(7) between t_{in} and the evaporation time $t_{\text{ev}} = \Gamma_{\text{BH}}^{-1}$, and using the relation (3), we obtain,

$$N_j^{m_j < T_{\text{BH}}^{\text{in}}} = \int_{t_{\text{in}}}^{t_{\text{ev}}} \frac{dN_j}{dt} = \frac{15g_j\zeta(3)}{g_*\pi^4} \frac{M_{\text{in}}^2}{M_{\text{P}}^2} \simeq 10^8 \left(\frac{M_{\text{in}}}{1\text{g}} \right)^2. \quad (8)$$

From the expression, a simple estimation suggests that a BH of mass 10 g can produce ~ 10 billion particles during its lifetime. Note that this result is valid for a scalar species j and should be multiplied by $\frac{3}{4}$ for a fermionic dark matter. The second distinct case arises, if $m_j \gtrsim T_{\text{BH}}^{\text{in}}$, and for such case one needs to integrate Eq.(7) between the time t_j to t_{ev} , where t_j corresponds to the time when the mass of the emitted particle satisfies $m_j = T_{\text{BH}}$. A straightforward calculation gives

$$t_j = \Gamma_{\text{BH}}^{-1} \left(1 - \frac{M_{\text{P}}^6}{m_j^3 M_{\text{in}}^3} \right), \quad (9)$$

and therefore, the total number of emitted particles turns out to be,

$$N_j^{m_j > T_{\text{BH}}^{\text{in}}} = \int_{t_j}^{t_{\text{ev}}} \frac{dN_j}{dt} = \frac{15g_j\zeta(3)}{g_*\pi^4} \frac{M_{\text{P}}^2}{m_j^2} \simeq 10^{14} \left(\frac{10^{10}\text{GeV}}{m_j} \right)^2. \quad (10)$$

We should also mention that the above result should be multiplied by $\frac{3}{4}$ for a fermionic dark matter.

To this end, a noticeable difference between the two distinct cases is worth summarizing. When the mass of the emitted particle is smaller than the black hole formation temperature, the total number of emitted particle $N_j \propto M_{\text{in}}^2$ solely depend on the PBH initial mass. Otherwise, the mass of the emitted particle controls $N_j \propto m_j^{-2}$ not the mass of the PBH.

C. Relic abundance

To obtain the dark matter (DM) relic abundance of the species j today at T_0 , we use [8],

$$\Omega_j h^2 = 1.6 \times 10^8 \frac{g_0}{g_{\text{RH}}} \frac{N_j \times n_{\text{BH}}(a_{\text{ev}})}{T_{\text{RH}}^3} \left(\frac{a_{\text{ev}}}{a_{\text{RH}}} \right)^3 \frac{m_j}{\text{GeV}}, \quad (11)$$

where $n_{\text{BH}} = \rho_{\text{BH}}/M_{\text{BH}}$ is the density of PBH. $g_{\text{RH}} = 106.75$ and $g_0 = 3.91$ are the effective number of light species for entropy at the end of reheating and present-day, respectively. We took both effective numbers of degrees of freedom for entropy and radiation is the same. Note that for $a_{\text{ev}} \geq a_{\text{RH}}$, the reheating being completed by PBHs, one sets $a_{\text{RH}} = a_{\text{ev}}$ in Eq.(11). One then needs to determine the PBH density $n_{\text{BH}}(a_{\text{ev}})$ as a function of the equation of state of the inflaton.

The PBH behaving like dust evolves as

$$\rho_{\text{BH}}(a_{\text{ev}}) = \beta \rho_\phi(a_{\text{in}}) \left(\frac{a_{\text{in}}}{a_{\text{ev}}} \right)^3 = 48\pi^2 \gamma^2 \beta \frac{M_P^6}{M_{\text{in}}^2} \left(\frac{a_{\text{in}}}{a_{\text{ev}}} \right)^3, \quad (12)$$

where we used Eq.(5) to write

$$\rho_\phi(a_{\text{in}}) = 48\pi^2 \gamma^2 \frac{M_P^6}{M_{\text{in}}^2}. \quad (13)$$

Considering that PBHs formed and evaporates during inflaton domination, we obtain

$$\begin{aligned} \left(\frac{a_{\text{in}}}{a_{\text{ev}}} \right)^3 &= \left(\frac{H_{\text{ev}}}{H_{\text{in}}} \right)^{\frac{2}{1+w_\phi}} = \left(\frac{2}{3(1+w_\phi)} \frac{\Gamma_{\text{BH}}}{H_{\text{in}}} \right)^{\frac{2}{1+w_\phi}} \\ &= \left(\frac{\epsilon}{2(1+w_\phi)\pi\gamma} \frac{M_P^2}{M_{\text{in}}^2} \right)^{\frac{2}{1+w_\phi}}, \end{aligned} \quad (14)$$

where we used Eqs.(4) and (5) for the last equality. Combining Eqs.(12) and (14) one obtains for $n_{\text{BH}}(a_{\text{ev}}) = \rho_{\text{BH}}(a_{\text{ev}})/M_{\text{BH}}$

$$n_{\text{BH}}(a_{\text{ev}}) = 48\pi^2 \beta \left(\frac{\gamma^{w_\phi} \epsilon}{2\pi(1+w_\phi)} \right)^{\frac{2}{1+w_\phi}} M_P^3 \left(\frac{M_P}{M_{\text{in}}} \right)^{\frac{7+3w_\phi}{1+w_\phi}}. \quad (15)$$

To compute the relic abundance (11), one needs to know the running between a_{ev} and a_{RH} which depends strongly on which system, PBHs or ϕ leads the reheating process. It is necessary to distinguish the two cases explicitly. Moreover, the PBH reheating can be achieved in two different regimes for β : if β is larger than a critical value β_c , given by [16]

$$\beta_c = \left(\frac{\epsilon}{(1+w_\phi)2\pi\gamma} \right)^{\frac{2w_\phi}{1+w_\phi}} \left(\frac{M_P}{M_{\text{in}}} \right)^{\frac{4w_\phi}{1+w_\phi}}, \quad (16)$$

PBHs dominate not only the reheating, but also the background dynamics over the inflaton, and evaporation takes place during PBH domination. On the other hand, if $\beta < \beta_c$, the PBH evaporates during inflaton domination

and can complete the reheating if $w_\phi > 1/3$, and the inflaton coupling with radiation field is smaller than some critical value² [16]. We will distinguish these four scenarios in detail in our following discussion.

D. PBH reheating

1. $\beta > \beta_c$

For $\beta > \beta_c$, the PBHs dominate the universe before their decay and complete the reheating independently of the inflaton system. As a consequence, the evaporation time *is* the reheating time, and $a_{\text{ev}} = a_{\text{RH}}$ in Eq.(11). The reheating temperature T_{RH} is given by the condition

$$\begin{aligned} H_{\text{RH}}^2 &= \frac{\rho_{\text{RH}}}{3M_P^2} = \frac{g_{\text{RH}}\pi^2 T_{\text{RH}}^4}{90M_P^2} = \frac{4\Gamma_{\text{BH}}^2}{9} \\ \Rightarrow T_{\text{RH}}^3 &= \frac{M_P^{\frac{15}{2}}}{M_{\text{in}}^{\frac{9}{2}}} \left(\frac{12\epsilon^2}{\alpha_T} \right)^{\frac{3}{4}}, \end{aligned} \quad (17)$$

where we used Eq.(4) and the fact that PBH decay happens in a dust-dominated Universe, $H(t_{\text{ev}}) = \frac{2}{3t_{\text{ev}}}$ and $\alpha_T = \frac{\pi^2}{30} g_{\text{RH}}$. However, in this scenario, PBHs are formed during inflaton domination, and the decay processes occur in PBH domination. Therefore, the relevant PBH mass evolution equation is

$$M_{\text{BH}}^3(a) \simeq M_{\text{in}}^3 - \frac{2\sqrt{3}\epsilon M_P^5}{\sqrt{\rho_\phi(a_{\text{BH}})}} \left(\frac{a}{a_{\text{BH}}} \right)^{\frac{3}{2}}, \quad (18)$$

where a_{BH} is the time when the PBH begins to dominate the energy budget, $\rho_\phi(a_{\text{BH}}) = \rho_{\text{BH}}(a_{\text{BH}})$. We assumed $M_{\text{BH}}(a_{\text{BH}}) \simeq M_{\text{in}}$ and $a \gg a_{\text{BH}}$. To obtain the scale factor associated with the evaporation point, one needs to solve

$$\begin{aligned} M(a_{\text{ev}}) = 0 &\Rightarrow \frac{a_{\text{ev}}}{a_{\text{BH}}} = \frac{M_{\text{in}}^2 \rho_\phi^{\frac{1}{3}}(a_{\text{BH}})}{(2\sqrt{3}\epsilon M_P^5)^{\frac{2}{3}}} \\ &= \frac{M_{\text{in}}^2 \rho_\phi^{\frac{1}{3}}(a_{\text{in}})}{(2\sqrt{3}\epsilon M_P^5)^{\frac{2}{3}}} \left(\frac{a_{\text{in}}}{a_{\text{BH}}} \right)^{(1+w_\phi)}. \end{aligned} \quad (19)$$

Using

$$\begin{aligned} \rho_\phi(a_{\text{BH}}) &= \rho_{\text{BH}}(a_{\text{BH}}) = \rho_\phi(a_{\text{in}}) \left(\frac{a_{\text{in}}}{a_{\text{BH}}} \right)^{3(1+w_\phi)} \\ &= \frac{1}{\beta} \rho_{\text{BH}}(a_{\text{in}}) \left(\frac{a_{\text{in}}}{a_{\text{BH}}} \right)^{3(1+w_\phi)}, \end{aligned} \quad (20)$$

² Note that in our analysis, we considered the inflaton reheating through its fermionic decay. Other processes have been studied in [13, 14] are left for future work.

we deduce

$$\frac{a_{\text{in}}}{a_{\text{BH}}} = \beta^{\frac{1}{3w_\phi}}, \quad (21)$$

and then, combining Eqs.(13), (19) and (21) we obtain

$$\frac{a_{\text{in}}}{a_{\text{ev}}} = \frac{a_{\text{in}}}{a_{\text{BH}}} \frac{a_{\text{BH}}}{a_{\text{ev}}} = \frac{1}{\beta^{\frac{1}{3}}} \left(\frac{\epsilon}{2\pi\gamma} \right)^{\frac{2}{3}} \left(\frac{M_p}{M_{\text{in}}} \right)^{\frac{4}{3}}. \quad (22)$$

Plugging Eq.(22) into (12), we obtain for the PBH number density at the evaporation point

$$n_{\text{BH}}(a_{\text{ev}}) = 12 \epsilon^2 \frac{M_P^{10}}{M_{\text{in}}^7}. \quad (23)$$

Combining Eq.(11) with Eqs.(8) and (23), we obtained for $m_j < T_{\text{BH}}^{\text{in}}$

$$\begin{aligned} \frac{\Omega_j h^2}{0.12} &= 4.2 \times 10^7 \frac{g_0 g_j}{\sqrt{g_*(T_{\text{BH}})} g_{RH}^{\frac{1}{4}}} \sqrt{\frac{M_P}{M_{\text{in}}}} \frac{m_j}{\text{GeV}} \\ &\simeq 4.9 \times 10^6 \sqrt{\frac{M_P}{M_{\text{in}}}} \frac{m_j}{\text{GeV}} \simeq \sqrt{\frac{10^8 \text{g}}{M_{\text{in}}}} \frac{m_j}{1 \text{ GeV}}, \end{aligned} \quad (24)$$

where we took $g_{RH} = g_*(T_{\text{BH}}) = 106.75$ and DM is scalar. We recognize from Eq.(24) the main feature we guessed in the introduction: for a given DM mass m_j , the relic abundance *decreases* for increasing values of M_{in} due to the lack of efficiency in the decay rate Γ_{BH} , Eq.(4). We also obtained the interesting result that for a 1 GeV dark matter, the right relic abundance is obtained for reasonable PBH masses of $M_{\text{in}} \sim 10^8$ g. We illustrate our results in Fig.(1), where we recognize the slope $m_j \propto \sqrt{M_{\text{in}}}$ in the bottom blue solid line in the plot, corresponding to the dependence obtained in Eq.(24) to achieve the right relic abundance. On the left of this line, too efficient PBH decay excludes a large region of the parameter space due to the overclosure of the Universe shown in green-shaded region. The pink-shaded regions indicate the forbidden window of PBH mass, which can disturb the BBN phase by introducing extra relativistic degrees of freedom. The minimum PBH mass obtained from the brown-shaded region is set by the maximum energy scale of inflation, which is constrained by the CMB observation.

For $m_j > T_{\text{BH}}^{\text{in}}$, the same exercise, using Eq.(10) instead of (8) gives

$$\begin{aligned} \frac{\Omega_j h^2}{0.12} &= 4.2 \times 10^7 \frac{g_0 g_j}{\sqrt{g_*(T_{\text{BH}})} g_{RH}^{\frac{1}{4}}} \frac{M_P^{\frac{9}{2}}}{M_{\text{in}}^{\frac{5}{2}} m_j^2} \frac{m_j}{\text{GeV}}, \\ &\simeq 4.9 \times 10^6 \frac{M_P^{\frac{9}{2}}}{M_{\text{in}}^{\frac{5}{2}} m_j^2} \frac{m_j}{\text{GeV}}, \end{aligned} \quad (25)$$

$$\simeq \left(\frac{10^8 \text{g}}{M_{\text{in}}} \right)^{\frac{5}{2}} \left(\frac{1.1 \times 10^{10} \text{GeV}}{m_j} \right). \quad (26)$$

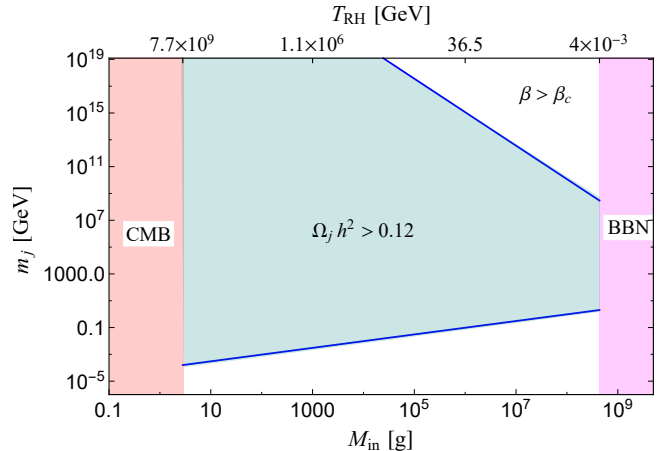


FIG. 1. Allowed region in the (M_{in}, m_j) and (T_{RH}, m_j) plane for $\beta > \beta_c$. BBN and CMB bounds exclude the magenta and red-shaded regions, respectively; see text for details.

We also recover the features we guessed in the introduction. For a given PBH population of mass M_{in} , the relic abundance *decreases* with m_j as the decay efficiency is largely reduced for heavy dark matter candidates, as it is clear from Eq.(10). We also observe this behavior on the top right of Fig.(1), where a viable region arises for large dark matter masses, following $m_j \propto M_{\text{in}}^{-5/2}$ as expected for a fixed relic abundance. One of the main results of our work is then that, in the case of PBH domination, the constraints on relic abundance allow only two very distinct regions: $10^{-5} \text{ GeV} \lesssim m_j \lesssim 1 \text{ GeV}$ (corresponding to $m_j \ll T_{\text{BH}}$), for which the upper and lower limits are set by BBN and CMB respectively. On the other hand, for $m_j \gg T_{\text{BH}}$, we obtained $M_P \gtrsim m_j \gtrsim 10^8 \text{ GeV}$, for which the lower limit is set by the BBN, and the upper limit is essentially the maximum possible mass that a fundamental particle can possibly possess namely the Planck mass.

2. $\beta < \beta_c$

If $\beta < \beta_c$, the PBHs decay *during* inflaton ϕ domination, and PBHs never dominate the energy budget of the Universe. However, for $w_\phi > 1/3$ and³ inflaton coupling below some critical value y_ϕ^c , PBH evaporation still determines the reheating temperature T_{RH} [16]. Writing the coupling between the inflaton and the radiation under the form $y_\phi \phi \bar{f} f$, one can estimate the expression for the critical coupling y_ϕ^c (given in the appendix-A). Similarly, once we fixed a particular coupling y_ϕ , there always ex-

³ The condition $w_\phi > 1/3$ ensures that the inflaton redshifts faster than the radiation.

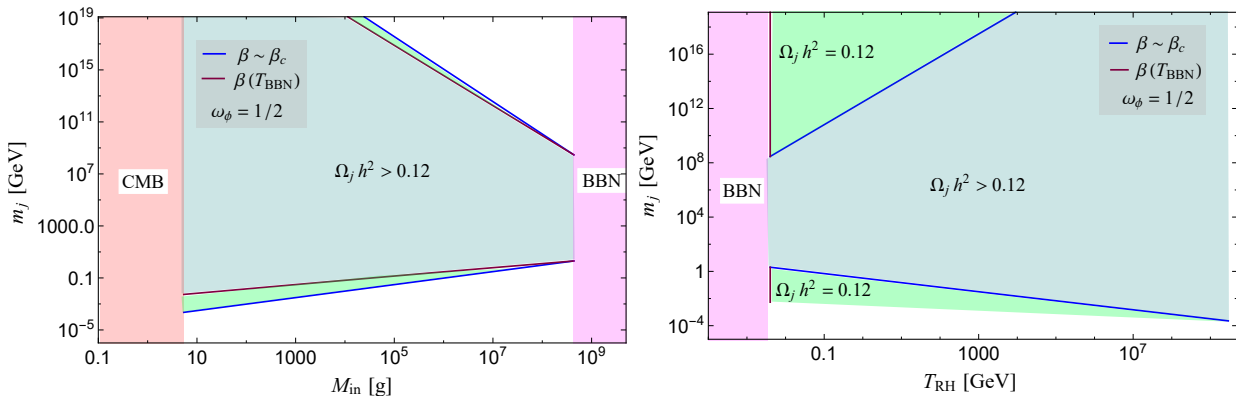


FIG. 2. Same as Fig.(1) for $\beta \leq \beta_c$. Here, the light green region indicates the allowed parameter space in the context of PBH reheating, with an inflaton coupling below the critical value $y_\phi \ll y_\phi^c$. We show two limiting values of β : the critical value β_c in blue below which the inflaton dominate the energy budget before the PBH decay and $\beta(T_{\text{BBN}}) < \beta_c$ in red which is the value of β for which the reheating temperature due to PBHs decay is the BBN bound $T_{\text{BBN}} = 4 \text{ MeV}$. The deep green region indicates DM overproduction.

ists a β value β_{BH} above which the PBHs determine the reheating temperature⁴.

However, there is a little subtlety here. The temperature generated by the PBH evaporation, T_{ev} , at a_{ev} is not strictly speaking the reheating temperature T_{RH} . However, as stated earlier, the Yukawa is too small ($y \ll y_\phi^c$) to affect the temperature of the thermal bath and T being reshifted from t_{ev} to t_{th} (time scale when $\rho_\phi = \rho_R$). Since dark matter and radiation production are concluded at the time of PBH evaporation, instead of Eq.(11), it is useful to use the following expression for the abundance,

$$\Omega_j h^2 = 1.6 \times 10^8 \frac{g_0}{g_{\text{RH}}} \frac{N_j \times n_{\text{BH}}(a_{\text{ev}})}{T_{\text{ev}}^3} \frac{m_j}{\text{GeV}}, \quad (27)$$

because the dominant temperature provided by the PBH decay follow a (quasi) iso-entropic law $T \propto a^{-1}$ between a_{ev} and a_{RH} .

The energy density of PBHs being transferred to the radiation at the evaporation time, one has $\rho_{\text{R}}(a_{\text{ev}}) = \rho_{\text{BH}}(a_{\text{ev}})$, or

$$\frac{n_{\text{BH}}(a_{\text{ev}})}{T_{\text{ev}}^3} = \left(\frac{\alpha_T^3 \rho_{\text{BH}}(a_{\text{ev}})}{M_{\text{in}}^4} \right)^{\frac{1}{4}}. \quad (28)$$

Implementing Eq.(28) in Eq.(27) using (12) and (14) one obtains for $m_j < T_{\text{BH}}^{\text{in}}$

$$\frac{\Omega_j h^2}{0.12} = 2.8 \times 10^8 \mu_j \beta^{\frac{1}{4}} \frac{g_0 g_j}{g_{\text{RH}}^{\frac{1}{4}} g_*(T_{\text{BH}})} \left(\frac{M_P}{M_{\text{in}}} \right)^{\frac{1-w_\phi}{2+2w_\phi}} \frac{m_j}{\text{GeV}}, \quad (29)$$

with

$$\mu_j = \left(\frac{\epsilon \pi^{w_\phi} \gamma^{w_\phi}}{2 + 2w_\phi} \right)^{\frac{1}{2+2w_\phi}} \quad (30)$$

whereas

$$\frac{\Omega_j h^2}{0.12} = 1.7 \times 10^{45} \mu_j \beta^{\frac{1}{4}} \frac{g_0 g_j}{g_{\text{RH}}^{\frac{1}{4}} g_*(T_{\text{BH}})} \left(\frac{M_P}{M_{\text{in}}} \right)^{\frac{5+3w_\phi}{2+2w_\phi}} \frac{\text{GeV}}{m_j}. \quad (31)$$

for $m_j > T_{\text{BH}}^{\text{in}}$. Note that we find similar expressions as Eqs.(24) and (25) if one sets $w_\phi = 0$. This is expected as for $w_\phi = 0$, the inflaton field behaves like dust, as PBH does.

We illustrate our result in Figs.(2), where we show the same parameter space as in the case of PBHs domination Fig.(1). To make the comparison easier, we have chosen two extreme parameters, $\beta = \beta_c$, corresponding to the preceding case, and $\beta = \beta(T_{\text{BBN}})$ corresponding to the case where the reheating temperature generated by the PBHs decay corresponds to the BBN temperature, $T_{\text{BBN}} \sim 4 \text{ MeV}$.

It is clear from Eqs.(29) and (31) that in this case, a new region of allowed parameter space opens up. Indeed, contrary to PBH domination, where only the lifetime of PBH (and not β) determined the relic abundance; here, along with the lifetime, the initial fraction also controls the abundance $\Omega_j h^2 \propto \beta^{\frac{1}{4}}$. In other words, for a given m_j , lowering β lowers the relic abundance, opening new allowed regions compared to the case $\beta \gtrsim \beta_c$. We represent these new regions in light green, for $w_\phi = \frac{1}{2}$ on the left panel of Fig.(2). Whereas the deep green region still overclose the Universe, the regions between the lines $\beta = \beta(T_{\text{BBN}})$ and $\beta = \beta_c$ possess the right relic abundance.

⁴ For very strong coupling y_ϕ such that inflaton completely decays before the completion of the evaporation process, we always required PBH domination ($\beta_{\text{BH}} \sim \beta_c$) to ensure PBH reheating.

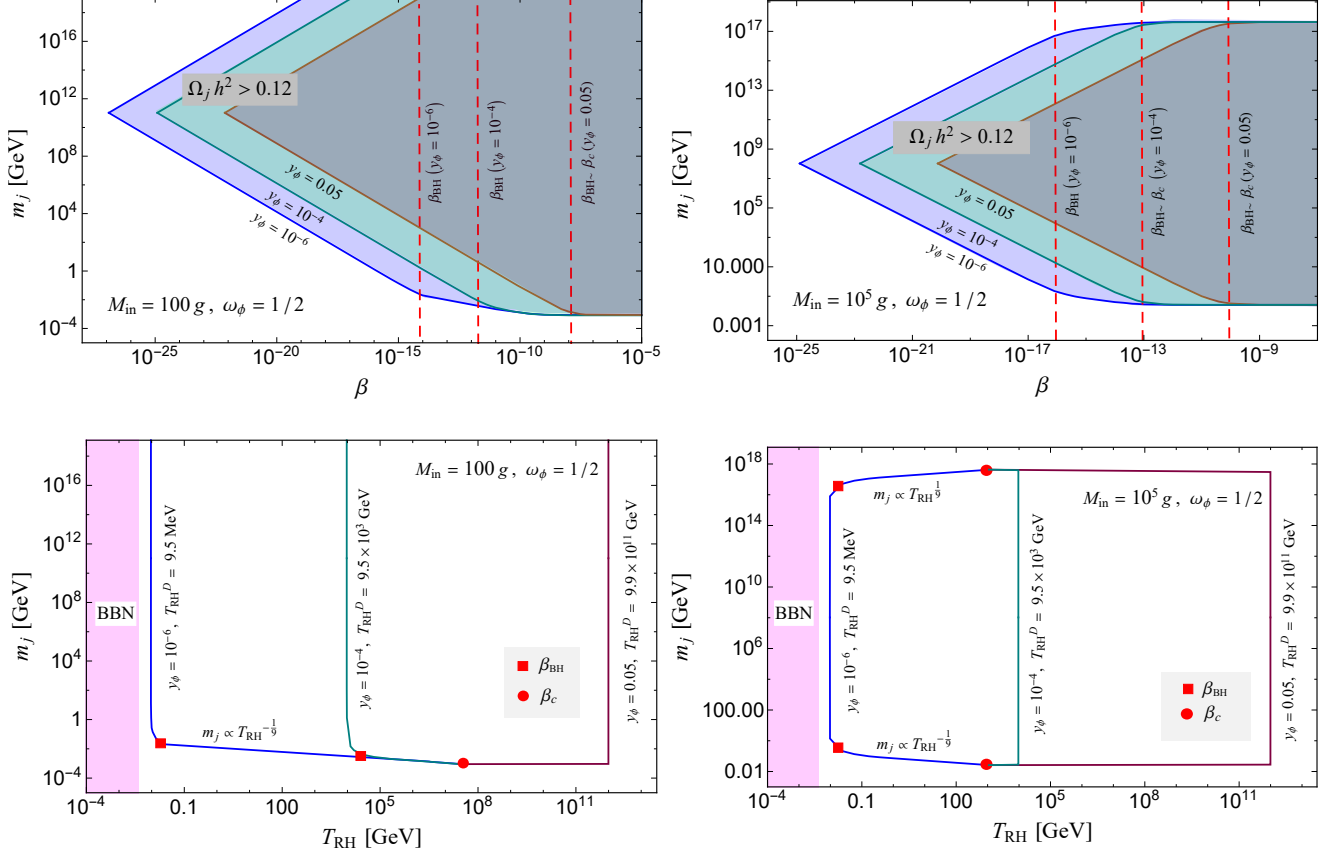


FIG. 3. Allowed parameter space for $w_\phi = 1/2$ in the (m_j, β) and (m_j, T_{RH}) plane for two different values of $M_{\text{in}} = (10^2, 10^5)$ g and three distinct values of $y_\phi = (0.05, 10^{-4}, 10^{-6})$. The shaded region in the upper panel plots indicates the forbidden regime due to overproduction. The vertical red dashed line indicates the divider line between the inflaton and PBH reheating. The regime on the right-hand side of the red dashed line is dominated by PBH reheating, whereas on the left-hand side, the Yukawa coupling y_ϕ defines the reheating temperature.

The slopes are given by Eq.(29) and (31), i.e. $m_j \propto \beta^{-\frac{1}{4}} M_{\text{in}}^{\frac{1-w_\phi}{2(1+w_\phi)}}$ for $m_j \ll T_{\text{BH}}^{\text{in}}$, and $m_j \propto \beta^{\frac{1}{4}} M_{\text{in}}^{-\frac{5+3w_\phi}{2(1+w_\phi)}}$ for $m_j \gg T_{\text{BH}}^{\text{in}}$. However, the reheating being completed by the PBHs population, the reheating temperature can also be expressed in terms of the fraction β as,

$$T_{\text{RH}} \sim M_P \beta^{\frac{3}{4} \frac{1+w_\phi}{3w_\phi-1}} \left(\frac{M_{\text{in}}}{M_P} \right)^{\frac{3}{2} \frac{1-w_\phi}{3w_\phi-1}}, \quad (32)$$

as shown in [16], also detailed in the Eq.(A12) of our dedicated appendix. Therefore, for a fixed value of reheating temperature, β behaves as proportional to $M_{\text{in}}^{-\frac{2(1-w_\phi)}{1+w_\phi}}$. Thus, $m_j \propto M_{\text{in}}^{\frac{1-w_\phi}{1+w_\phi}}$ for $m_j \ll T_{\text{BH}}^{\text{in}}$, and $m_j \propto M_{\text{in}}^{-\frac{3+w_\phi}{1+w_\phi}}$ for $m_j \gg T_{\text{BH}}^{\text{in}}$. For $w_\phi = \frac{1}{2}$, this corresponds to slopes $m_j \propto M_{\text{in}}^{\frac{1}{3}}$ for $m_j \ll T_{\text{BH}}^{\text{in}}$, and $m_j \propto M_{\text{in}}^{-\frac{7}{3}}$ for $m_j \gg T_{\text{BH}}^{\text{in}}$, which is effectively what is observed on the red lines in the left panel of Fig.(2) where we fixed the reheating temperature to be $T_{\text{RH}} = T_{\text{BBN}}$.

We show in the right panel of Fig.(2) the same analysis but in the (T_{RH}, m_j) -plane. This is just another representation of our results. Indeed, combining Eqs.(32) and (29) or (31), for each couple (T_{RH}, m_j) , there exists a unique couple (β, M_{in}) which fixes T_{RH} and $\Omega_j h^2$. We obtain $m_j \propto T_{\text{RH}}^{\frac{3w_\phi-1}{3(1+w_\phi)}}$ for a fixed value of $\beta < \beta_c$ when $m_j \ll T_{\text{BH}}^{\text{in}}$ and $m_j \propto T_{\text{RH}}^{-\frac{(3w_\phi-1)(5+3w_\phi)}{(1+w_\phi)(1-w_\phi)}}$ for $m_j \gg T_{\text{BH}}^{\text{in}}$. For example, for $w_\phi = \frac{1}{2}$ and any fixed value of β , $m_j \propto T_{\text{RH}}^{\frac{1}{9}}$ for $m_j \ll T_{\text{BH}}^{\text{in}}$ and $m_j \propto T_{\text{RH}}^{-\frac{13}{3}}$ for $m_j \gg T_{\text{BH}}^{\text{in}}$. Similarly, for a fixed M_{in} , we have $m_j \propto T_{\text{RH}}^{\frac{1-3w_\phi}{3(1+w_\phi)}}$ for $m_j \ll T_{\text{BH}}^{\text{in}}$ and $m_j \propto T_{\text{RH}}^{\frac{3w_\phi-1}{3(1+w_\phi)}}$ for $m_j \gg T_{\text{BH}}^{\text{in}}$, which gives for $w_\phi = \frac{1}{2}$, $m_j \propto T_{\text{RH}}^{-\frac{1}{9}}$ for $m_j \ll T_{\text{BH}}^{\text{in}}$ and $m_j \propto T_{\text{RH}}^{\frac{1}{9}}$ for $m_j \gg T_{\text{BH}}^{\text{in}}$ (see, for instance, lower panel of Fig.(3)).

E. Inflaton reheating

If $\beta < \beta_c$ and the inflaton coupling is strong enough, $y_\phi \gtrsim y_\phi^c$, the inflaton dominates the reheating process *and also* determines T_{RH} . However, depending on the coupling strength, the reheating, which is governed by the inflaton decay width Γ_ϕ may happen before or after the evaporation point a_{ev} . We give in the appendix-B the threshold value y_ϕ^{th} above which the inflaton decays before the PBH evaporates as a function of the parameters of the inflationary potential $V(\phi)$.

Note that in our analysis, we always supposed that the PBHs are formed *during* the reheating, which means $a_{\text{in}} < a_{\text{RH}}$. Following the same procedure as in the previous section, we will discuss in details the two possibilities.

1. $a_{\text{ev}} < a_{\text{RH}}$

If $y_\phi^c < y_\phi < y_\phi^{\text{th}}$, the PBHs evaporate before the end of reheating thus, $a_{\text{ev}} < a_{\text{RH}}$. The dilution of the dark component between a_{ev} and a_{RH} is then modified compared to our previous analysis due the injection of a considerable amount of entropy during the decay of the inflaton, which was negligible in the previous section. This injection can considerably dilute the relic abundance, and we expect an increase in the allowed mass range, allowing heavier dark matter. Whereas N_j is not modified by the presence of the inflaton, $n_{\text{BH}}(a_{\text{ev}}) (a_{\text{ev}}/a_{\text{RH}})^3$ appearing in Eq.(11) is affected. Connecting the evolution of the scale factor from the evaporation point to the reheating time in the inflaton-dominated era, we obtain

$$\begin{aligned} \frac{a_{\text{ev}}}{a_{\text{RH}}} &= \left(\frac{t_{\text{ev}}}{t_{\text{RH}}} \right)^{\frac{2}{3(1+w_\phi)}} = \left(\frac{3(1+w_\phi) H_{\text{RH}}}{2 \Gamma_{\text{BH}}} \right)^{\frac{2}{3(1+w_\phi)}} \\ &= \left(\frac{(1+w_\phi) \sqrt{\alpha_T} T_{\text{RH}}^2 M_{\text{in}}^3}{2\sqrt{3} M_P \epsilon M_P^4} \right)^{\frac{2}{3(1+w_\phi)}}. \end{aligned} \quad (33)$$

The number density of the species j at a_{RH} is then given by Eq.(15) modulo the dilution factor between a_{ev} and a_{RH}

$$n_j(a_{\text{RH}}) = N_j \times n_{\text{BH}}(a_{\text{ev}}) \times \left(\frac{\sqrt{\alpha_T} (1+w_\phi) T_{\text{RH}}^2 M_{\text{in}}^3}{2\sqrt{3} \epsilon M_P^5} \right)^{\frac{2}{1+w_\phi}}. \quad (34)$$

Utilizing Eq.(34) one obtains the ratio

$$\frac{n_j(a_{\text{RH}})}{T_{\text{RH}}^3} = \tilde{\mu} \left(\frac{M_P^{4w_\phi-2} M_{\text{in}}^{1-w_\phi}}{T_{\text{RH}}^{3w_\phi-1}} \right)^{\frac{1}{1+w_\phi}}, \quad (35)$$

for $m_j < T_{\text{BH}}^{\text{in}}$ with

$$\tilde{\mu} = \frac{720 g_j \zeta(3) \beta}{g_*(T_{\text{BH}}) \pi^2} \left(\frac{\sqrt{\alpha_T} \gamma^{w_\phi}}{4\sqrt{3} \pi} \right)^{\frac{2}{1+w_\phi}}. \quad (36)$$

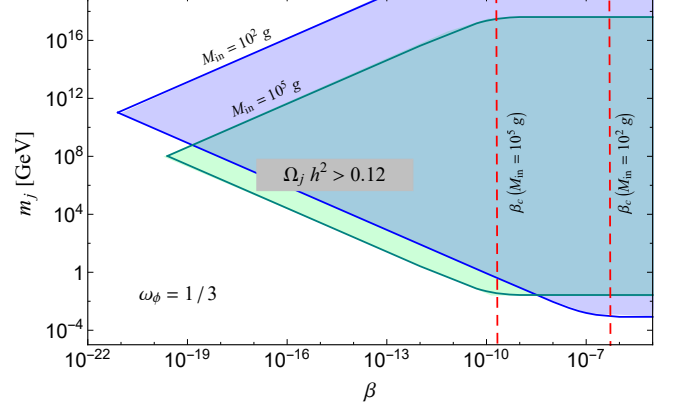


FIG. 4. Allowed parameter space for $w_\phi = 1/3$ in the (m_j, β) plane for two different values of $M_{\text{in}} = (10^2, 10^5)$ g. Interestingly, once we fixed M_{in} , (m_j, β) parameter space turns out to be independent of coupling value y_ϕ .

This gives for $g_{\text{RH}} = g_*(T_{\text{BH}}) = 106.75$,

$$\begin{aligned} \frac{\Omega_j h^2}{0.12} &= 4.9 \times 10^7 \tilde{\mu} \left(\frac{M_P^{4w_\phi-2} M_{\text{in}}^{1-w_\phi}}{T_{\text{RH}}^{3w_\phi-1}} \right)^{\frac{1}{1+w_\phi}} \frac{m_j}{1 \text{ GeV}} \\ &\simeq 3.4 \times 10^6 \beta \left(\frac{M_P^{4w_\phi-2} M_{\text{in}}^{1-w_\phi}}{T_{\text{RH}}^{3w_\phi-1}} \right)^{\frac{1}{1+w_\phi}} \frac{m_j}{1 \text{ GeV}} \quad (37) \\ &\simeq 3.4 \times 10^6 \beta \left(\frac{M_{\text{in}}}{M_P} \right)^{\frac{1-w_\phi}{1+w_\phi}} \left(\frac{M_P}{T_{\text{RH}}} \right)^{\frac{3w_\phi-1}{1+w_\phi}} \frac{m_j}{1 \text{ GeV}}. \end{aligned}$$

For $m_j > T_{\text{BH}}^{\text{in}}$, we obtain

$$\frac{n_j(a_{\text{RH}})}{T_{\text{RH}}^3} = \frac{\tilde{\mu}}{m_j^2} \left(\frac{M_P^{2+8w_\phi}}{M_{\text{in}}^{1+3w_\phi} T_{\text{RH}}^{3w_\phi-1}} \right)^{\frac{1}{1+w_\phi}}, \quad (38)$$

and

$$\begin{aligned} \frac{\Omega_j h^2}{0.12} &= 4.9 \times 10^7 \frac{\tilde{\mu}}{m_j^2} \left(\frac{M_P^{2+8w_\phi}}{M_{\text{in}}^{1+3w_\phi} T_{\text{RH}}^{3w_\phi-1}} \right)^{\frac{1}{1+w_\phi}} \frac{m_j}{1 \text{ GeV}} \\ &\simeq 3.4 \times 10^6 \frac{\beta}{m_j^2} \left(\frac{M_P^{2+8w_\phi}}{M_{\text{in}}^{1+3w_\phi} T_{\text{RH}}^{3w_\phi-1}} \right)^{\frac{1}{1+w_\phi}} \frac{m_j}{1 \text{ GeV}} \quad (39) \\ &\simeq 2 \times 10^{30} \beta \left(\frac{M_P}{M_{\text{in}}} \right)^{\frac{1+3w_\phi}{1+w_\phi}} \left(\frac{M_P}{T_{\text{RH}}} \right)^{\frac{3w_\phi-1}{1+w_\phi}} \frac{10^{13} \text{ GeV}}{m_j}. \end{aligned}$$

2. $a_{\text{ev}} > a_{\text{RH}}$

For even stronger inflaton coupling $y_\phi > y_\phi^{\text{th}} > y_\phi^c$, there exists the possibility that the inflaton decays even

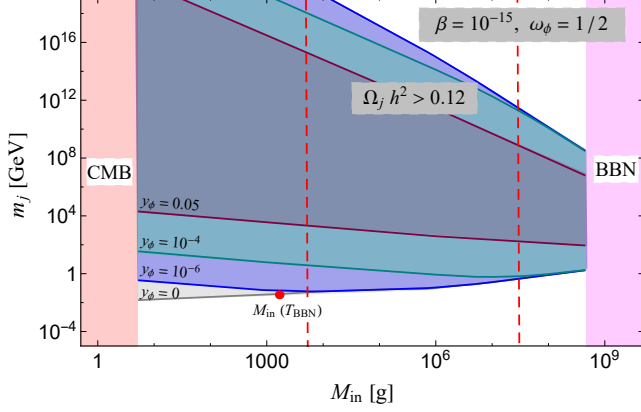


FIG. 5. Allowed region in the (M_{in}, m_j) plane for four different values of the coupling $y_\phi = (0.05, 10^{-4}, 10^{-6}, 0)$ with $w_\phi = \frac{1}{2}$ and $\beta = 10^{-15}$. BBN and CMB bounds exclude the magenta and red-shaded regions, respectively. For each value of y_ϕ , the vertical red dashed lines (left one is for $y_\phi = 10^{-6}$ and the right one is for $y_\phi = 10^{-4}$) separate the regions between the inflaton and PBH reheating. The regions on the right side of the red dashed lines are dominated by PBH reheating, whereas on the left-side, the Yukawa reheating temperature is determined by y_ϕ . The red circle represents the PBH formation mass associated with the case where reheating temperature from the PBH decay corresponds to the BBN temperature and here we set coupling $y_\phi = 0$.

before the completion of the PBH evaporation process. In other words, $a_{\text{ev}} > a_{\text{RH}}$. In this case, we have

$$\begin{aligned} \frac{n_j(a_{\text{ev}})}{T^3(a_{\text{ev}})} &= \frac{N_j \times n_{\text{BH}}(a_{\text{ev}})}{T^3(a_{\text{ev}})} = N_j \frac{n_{\text{BH}}(a_{\text{in}}) \left(\frac{a_{\text{in}}}{a_{\text{ev}}}\right)^3}{T_{\text{RH}}^3 \left(\frac{a_{\text{RH}}}{a_{\text{ev}}}\right)^3} \\ &= N_j \times \frac{48\pi^2 \gamma^2 \beta \frac{M_P^6}{M_{\text{in}}^3} \left(\frac{a_{\text{in}}}{a_{\text{RH}}}\right)^3}{T_{\text{RH}}^3}, \end{aligned} \quad (40)$$

where we supposed that no particles had decoupled from the thermal plasma between a_{RH} and a_{ev} , and used Eq.(13). The scale factor between the formation and reheating point can be connected through the evolution of the Hubble parameter as,

$$\frac{a_{\text{in}}}{a_{\text{RH}}} = \left(\frac{H_{\text{RH}}}{H_{\text{in}}}\right)^{\frac{2}{3(1+w_\phi)}} = \left(\sqrt{\frac{\alpha_T}{3}} \frac{M_{\text{in}} T_{\text{RH}}^2}{4\pi\gamma M_P^3}\right)^{\frac{2}{3(1+w_\phi)}}, \quad (41)$$

where H_{RH} is the Hubble parameter at the end of reheating.

Implementing Eq.(41) into Eq.(40), one can find the ratio

$$\frac{n_j(a_{\text{ev}})}{T^3(a_{\text{ev}})} = \tilde{\mu} \left(\frac{M_P^{4w_\phi-2} M_{\text{in}}^{1-w_\phi}}{T_{\text{RH}}^{3w_\phi-1}}\right)^{\frac{1}{1+w_\phi}}, \quad (42)$$

for $m_j < T_{\text{BH}}^{\text{in}}$ and for $m_j > T_{\text{BH}}^{\text{in}}$

$$\frac{n_j(a_{\text{ev}})}{T^3(a_{\text{ev}})} = \frac{\tilde{\mu}}{m_j^2} \left(\frac{M_P^{2+8w_\phi}}{M_{\text{in}}^{1+3w_\phi} T_{\text{RH}}^{3w_\phi-1}}\right)^{\frac{1}{1+w_\phi}}, \quad (43)$$

Interestingly above equations (42) and (43) turn out to be exactly the same with the previous case $a_{\text{RH}} > a_{\text{ev}}$ (see, for instance, Eq.(35) and (38)). Therefore, the DM abundance naturally follows Eqs.(37) and (39). An easier way to understand this is to notice that the present relic abundance is given by

$$n_j(a_0) = n_j(a_{\text{ev}}) \left(\frac{a_{\text{ev}}}{a_0}\right)^3 = n_{\text{BH}}(a_{\text{ev}}) N_j \left(\frac{a_{\text{ev}}}{a_0}\right)^3,$$

which gives

$$\begin{aligned} n_j(a_0) &= n_{\text{BH}}(a_{\text{in}}) N_j \left(\frac{a_{\text{in}}}{a_0}\right)^3 \\ &= n_{\text{BH}}(a_{\text{in}}) N_j \left(\frac{a_{\text{in}}}{a_{\text{RH}}}\right)^3 \left(\frac{a_{\text{RH}}}{a_0}\right)^3. \end{aligned}$$

If the dilution is dominated by the same field (in this case the inflaton) between a_{in} and a_{RH} , the relic abundance does not depend on the evaporation time.

We show in the upper panel of Fig.(3) the allowed regions in the (β, m_j) parameter space for different values of y_ϕ and $M_{\text{in}} = 100$ g (left) or 10^5 g (right) with $w_\phi = \frac{1}{2}$. For each y_ϕ , we also plotted in the same figure the lines for β_{BH} , corresponding to the value of β above which the PBHs dominate the reheating process over the inflaton. On the left side of the β_{BH} line, the inflaton reheats the Universe, and we recover the behavior we found in Eqns.(37) and (39) i.e. points allowed by the relic density constraint respects $m_j \propto \frac{1}{\beta}$ for $m_j \ll T_{\text{BH}}^{\text{in}}$ and $m_j \propto \beta$ for $m_j \gg T_{\text{BH}}^{\text{in}}$. Once $\beta > \beta_{\text{BH}}$, m_j follows the law $m_j \propto \beta^{-\frac{1}{4}}$ for $m_j \ll T_{\text{BH}}^{\text{in}}$ ($\beta^{\frac{1}{4}}$ for $m_j \gg T_{\text{BH}}^{\text{in}}$) as expected from Eq.(29) and (31). Then, once $\beta \gtrsim \beta_c$, the relic density depends only on the PBH lifetime and is then independent on β , as we also noticed on Eq.(24). We also show our result in the plane (T_{RH}, m_j) in the lower panel. To this end, it may indeed be worth pointing the special case at $w_\phi = 1/3$, for which DM abundance turns independent of T_{RH} or inflaton coupling y_ϕ . For such case, also we showed the behavior in (β, m_j) plane in Fig.(4). Due to the indistinguishable nature between the inflaton and radiation, the intermediate $m_j \propto \beta^{\pm 1/4}$ behavior corresponding to PBH reheating does not arise, and hence $\beta_{\text{BH}} = \beta_c$ condition satisfies as expected.

Finally, for clear comparison with the two preceding cases (PBH reheating and domination, PBH reheating and inflaton domination) we plotted in Fig.(5) the allowed region in the (M_{in}, m_j) plane for $w_\phi = \frac{1}{2}$ and different values of y_ϕ . We clearly see that increasing y_ϕ exclude region shrinks naturally. Indeed, for inflaton domination,

the reheating temperature increases with y_ϕ . As a consequence, the same amount of relic abundance is obtained for *higher* dark matter mass in the case $m_j < T_{\text{BH}}^{\text{in}}$ as one can see from Eq.(37). For $m_j > T_{\text{BH}}^{\text{in}}$, it is the opposite, see Eq.(39), and a *lower* DM mass is necessary to obtain the right amount of relic abundance. This is easy to understand, as higher reheating temperature there is a tendency to dilute the dark matter abundance more. What is also interesting in this plot is the different regimes that can be observed for M_{in} . For very large values of M_{in} , not far from the BBN limit, the reheating is determined by the PBH while they dominate the Universe, and we recover the results showed in Fig.(1). For intermediate values of M_{in} , the PBHs do not dominate the Universe but dominate the reheating process, whereas for low M_{in} , on the left side of the dashed lines, the PBHs dominate neither the Universe's energy budget nor the reheating process. In this case, the dependence between M_{in} and m_j changes slope between these two regimes, as we can see comparing Eqs.(29) and (37). It is easy to understand, as in the case of inflaton reheating, lower values of M_{in} produces less dark matter particles, see Eq.(8), and then necessitates higher dark matter masses. The situation is the opposite for intermediate value of M_{in} when PBH dominates the reheating because of the dilution effect described by Eq.(28).

III. REFINEMENTS

A. The case for extended mass distribution

Depending on the underlying mechanism that governs their formation, PBHs may exhibit extended mass distribution that is contingent on the power spectrum of primordial density perturbations and the equation of state of the Universe at the time of their formation (see Ref. [47]), for example power-law [48], log-normal [49–51], critical collapse [52–55], or metric preheating [56–58], among others. In the current section, we consider the class PBHs with power-law shape mass function of the form:

$$f_{\text{PBH}}(M_i, t_i) = \begin{cases} CM_i^{-\alpha}, & \text{for } M_{\text{min}} \leq M_i \leq M_{\text{max}} \\ 0, & \text{otherwise,} \end{cases} \quad (44)$$

where t_i and coefficient C are respectively the initial time and the overall normalization factor. M_{min} and M_{max} represent the minimum and the maximum PBH masses, respectively. We parameterize the width of PBHs masses range by two parameters M_{in} and σ , such that $M_{\text{min}} = M_{\text{in}}10^{-\sigma}$ and $M_{\text{max}} = M_{\text{in}}$. The parameter $\alpha = \frac{2+4\omega_\phi}{1+\omega_\phi}$ (see Ref. [16, 32]).

Then the evolution equations for ρ_{BH} and ρ_R become:

$$\begin{aligned} \frac{d\rho_R}{da} + 4\frac{\rho_R}{a} &= \frac{\Gamma_\phi \rho_\phi (1 + w_\phi)}{aH} \\ &\quad - \frac{a^3}{a_{\text{in}}^3} \int_{\widetilde{M}}^{\infty} \frac{dM}{da} f_{\text{PBH}}(M_i, t_i) dM_i \\ \frac{d\rho_{\text{BH}}}{da} + 3\frac{\rho_{\text{BH}}}{a} &= \frac{a^3}{a_{\text{in}}^3} \int_{\widetilde{M}}^{\infty} \frac{dM}{da} f_{\text{PBH}}(M_i, t_i) dM_i \end{aligned} \quad (45)$$

where the lower bound \widetilde{M} allows to ensure that at time t only the non-evaporated PBHs with mass M_i larger than \widetilde{M} contribute to the energy density, and is given by:

$$\widetilde{M}(a) = \left(\frac{2\sqrt{3}\epsilon}{1 + \omega_\phi} \right)^{1/3} \left(\frac{M_P^5}{\sqrt{\rho_{\text{end}}}} \right)^{1/3} \left(\frac{a}{a_{\text{in}}} \right)^{\frac{1}{2}(1 + \omega_\phi)}. \quad (46)$$

In this scenario, we employed a modified version of the package called **FRISBHEE** [32–34, 59]. This modified version incorporated the inflaton into the evolving system, enabling us to solve a set of evolution equations and calculate the relic abundance. This approach is necessary due to the intricacies introduced by the presence of integrals on the right-hand side of Eq.(45), which makes the situation somewhat more complex than the monochromatic scenario.

Before presenting the results, let's recall that the reheating through PBHs, after a regime of PBH domination, happens when they completely evaporate. Hence, as shown in [16], the choice of the mass function that extends to lower values, with the maximal initial mass M_{max} corresponding to the monochromatic mass M_{in} , guarantees that the complete evaporation of PBHs in both cases is achieved at the same epoch. Therefore the reheating temperature would be somewhat same in both cases for a given M_{in} .

Our findings yield similar results for both the extended and monochromatic PBH mass spectra, as depicted in Fig.(6), under the conditions of $\beta > \beta_c$ and $\sigma = 2$, which corresponds to the range $M_{\text{in}} \in [10^6, 10^8]$ g. Nevertheless, certain distinctions are noteworthy.

We observe that in the light DM mass region, $m_j < T_{\text{BH}}^{\text{in}}$, there is no substantial difference between the monochromatic and extended cases as can be seen in lower line of Fig.(6). This happens because the number of DM particles produced is $\propto (M_{\text{in}})^2$, and so the dominant contribution comes from heaviest PBH, which in our case corresponds to monochromatic mass.

However, in the high DM mass region, $m_j > T_{\text{BH}}^{\text{in}}$, there is a substantial difference. First, the number density of DM is larger compared with the monochromatic case because not only the largest mass M_{in} produces DM particles, but as soon as the lighter population of PBHs start to evaporate, they will produce DM particles $\propto (m_j)^{-2}$ as well. Consequently a much wider parameter space of m_j is excluded. The exclusion region for a given M_{in} would

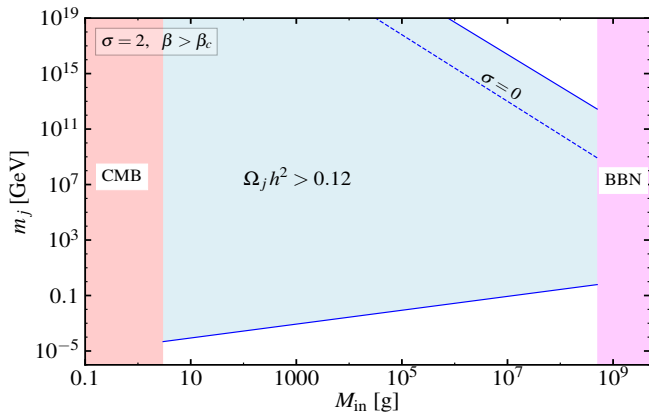


FIG. 6. Allowed region in the (M_{in}, m_j) plane for $\beta > \beta_c$ in the case of the power-law extended mass distribution, with $\sigma = 2$ (see text for details). The dashed blue line correspond to the monochromatic ($\sigma = 0$) scenario. BBN and CMB bounds exclude the magenta and red-shaded regions, respectively.

be similar to that of the monochromatic scenario when the PBH initial mass $\gtrsim M_{\text{in}} 10^{-\sigma}$. This can be observed in Fig.(6) where, for example, for $M_{\text{in}} \sim 10^8 \text{g}$ and $\sigma = 2$, avoiding overproduction of DM requires $m_j \gtrsim 10^{14} \text{GeV}$, corresponding to roughly to the excluded region for the monochromatic case ($\sigma = 0$) when $M_{\text{in}} \sim 4 \times 10^6 \text{g}$ as can be deduced from the upper dashed blue line.

In light of these results, some comments are in order: the exclusion region for m_j strongly dependent on the size of the width of the distribution, in such a way the larger the σ , the stronger the constrain on m_j , that is the larger, the mass of DM particles is necessary to not overproduce it. We also note that if the distribution extends to larger masses such that $M_{\text{in}} = M_{\text{min}}$, the reheating temperature, and the DM number density, can be very affected depending on the width of the mass function, since the larger masses than M_{in} would have larger lifetime compared to the monochromatic scenario. This will affect both the low and high DM mass regimes.

B. Limit on the DM mass from warm dark matter (WDM) constraints

1. Generalities

The DM from PBH evaporation has a large initial momentum. Higher initial momentum indicates a large free streaming length, which might erase small-scale structures. Indeed, if boosted at production time, the classical limit on warm dark matter ($m_j \gtrsim 3 \text{keV}$) coming from structure formation or Lyman- α constraints needs to be revisited. The idea is simple. A straightforward calculation shows that the free streaming length λ_{FS} can

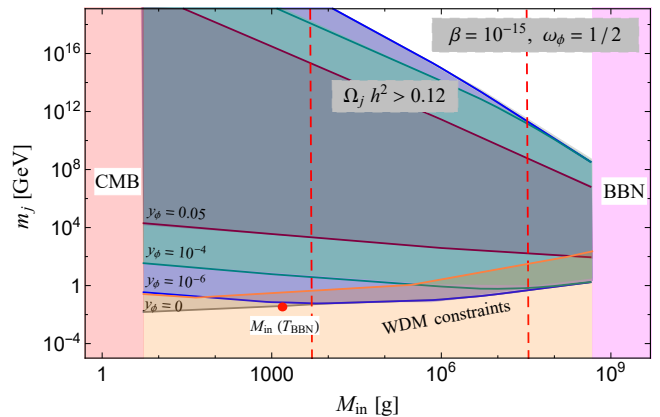


FIG. 7. Same as Fig.(5) taking into account the restriction from the warm dark matter constraint (orange shaded region).

be approximated by [8]

$$\lambda_{FS} \simeq 70 \text{ Mpc} \frac{1 \text{ eV}}{T_{nr}}, \quad (47)$$

where T_{nr} is the temperature at the time when the DM becomes non-relativistic, or $p \gtrsim m_j$, p is the momentum of the DM. If $p \sim T$ at production time, because T and p redshifts as a^{-1} , the condition can indeed be read $T_{nr} \sim m_j$, and the classical limits apply. This is the typical case for WIMP or FIMP candidates. However, if the dark matter momentum p is boosted by a process at production time, $p = \gamma T$, with $\gamma \gg 1$ the condition $p \sim m_j$ becomes $T_{nr} \sim \frac{m_j}{\gamma}$, and Eq.(47) becomes

$$\lambda_{FS} \simeq 70 \text{ Mpc} \frac{1 \text{ eV}}{m_j} \gamma, \quad (48)$$

transforming the condition from $m_j \gtrsim 3 \text{keV}$ to $m_j \gtrsim 3 \gamma \text{keV}$. This is exactly what is happening in the case of production from PBH evaporation because the dark matter momentum at evaporation $p_{\text{ev}} \sim T_{\text{BH}}^{\text{in}} \gg T_{\text{RH}}$. We propose to study in more detail each cases analyzed previously in this context.

2. $\beta > \beta_c$

Since DM particles have no interaction with other particles from the evaporation point to the present day we have momentum value at the present day

$$p_0 = \frac{a_{\text{ev}}}{a_0} p_{\text{ev}} = \frac{a_{\text{ev}}}{a_{\text{eq}}} \frac{\Omega_{\text{R}}}{\Omega_{\text{m}}} p_{\text{ev}} \quad (49)$$

where at present-day radiation relic abundance $\Omega_{\text{R}} = 5.4 \times 10^{-5}$ and matter relic abundance $\Omega_{\text{m}} \simeq 0.315$. a_{eq} and a_{ev} are the scale factor at the radiation-matter equality and evaporation point, respectively. In the limit,

$\beta > \beta_c$, PBH evaporation completes during PBH domination, and comoving entropy density is conserved from the end of the evaporation point to the present day. In this context, $T_{\text{ev}} = T_{\text{RH}}$ and using entropy conservation, p_0 can be rewritten as

$$p_0 = \left[\frac{g_{\text{eq}}^s}{g_{\text{RH}}^s} \right]^{1/3} \frac{T_{\text{eq}}}{T_{\text{RH}}} \frac{\Omega_R}{\Omega_m} p_{\text{ev}}, \quad (50)$$

where g_{RH}^s and g_{eq}^s represent the effective degrees of freedom for entropy at the end of reheating and radiation-matter equality, respectively. $T_{\text{eq}} = 0.8$ eV is the radiation temperature at radiation-matter equality. In the case of light DM, $m_j \ll T_{\text{BH}}^{\text{in}}$, the average momentum of the light DM matter particle radiated by a PBH, $p_{\text{ev}} \sim T_{\text{BH}}^{\text{in}}$. Moreover, the usual velocity of the warm DM at present, which decoupled while they are relativistic, is assumed to be [40]

$$v_{\text{WDM}} \simeq 3.9 \times 10^{-8} \left(\frac{\text{keV}}{m_{\text{WDM}}} \right)^{3/4}. \quad (51)$$

Several experiments put constraints on the WDM, such as HIRES/MIKE Lyman- α forest data sets and XQ-100, the MCMC analysis restricts WDM mass $m_{\text{WDM}} > 5.3$ keV at 2σ range [41]. In references [42, 43], using HIRES/MIKE, the authors obtained the bound on WDM $m_{\text{WDM}} > 3.3$ keV and > 3.95 keV using SDSSIII/BOSS. Throughout our analysis, we choose the restriction on the mass of the WDM, $m_{\text{WDM}} > 3.3$ keV. Now utilizing the above equations (50) and (51) together with (17), one can find

$$\frac{m_j}{\text{GeV}} \geq 7 \times 10^{-7} \left(\frac{m_{\text{WDM}}}{\text{keV}} \right)^{4/3} \left(\frac{M_{\text{in}}}{M_P} \right)^{1/2}, \quad (52)$$

where $m_{\text{WDM}} \sim 3.3$ keV. For example, if one takes 10 g of initial PBH mass, the DM mass bound turns out to be $m_j > 5.2 \times 10^{-3}$ GeV. Note that this bound does not depend on the inflaton EoS and PBH fraction as expected. We also recover the naive constraint we obtained previously remarking that the boost factor $\gamma = \frac{p_{\text{ev}}}{T_{\text{RH}}} \sim \frac{T_{\text{BH}}^{\text{in}}}{T_{\text{RH}}} \sim \sqrt{\frac{M_{\text{in}}}{M_P}}$.

3. $\beta < \beta_c$ (PBH reheating)

In the limit $\beta < \beta_c$, if the coupling value $y_\phi < y_\phi^c$, PBH decay determines reheating temperature. Thus, after the evaporation point to the present day, the comoving entropy energy density is conserved, and the expression for p_0

$$p_0 = \left[\frac{g_{\text{eq}}^s}{g_{\text{ev}}^s} \right]^{1/3} \frac{T_{\text{eq}}}{T(a_{\text{ev}})} \frac{\Omega_R}{\Omega_m} \frac{M_P^2}{M_{\text{in}}}, \quad (53)$$

where g_{ev}^s represents the effective degrees of freedom for entropy at the end of evaporation. In this scenario, PBH evaporates during inflaton domination, and evaporation temperature can be calculated from $\rho_{\text{BH}}(a_{\text{ev}})$ (see, for instance, Eq.(15))

$$T(a_{\text{ev}}) \simeq \left(\frac{\rho_{\text{BH}}}{\alpha_T} \right)^{1/4} = \left(\frac{48\pi^2 \beta}{\alpha_T} \right)^{1/4} \tilde{\mu}_1 M_P \left(\frac{M_P}{M_{\text{in}}} \right)^{\frac{3+w_\phi}{2(1+w_\phi)}}, \quad (54)$$

where $\tilde{\mu}_1 = \left(\frac{\gamma^{w_\phi} \epsilon}{2\pi(1+w_\phi)} \right)^{\frac{1}{2(1+w_\phi)}}$. Utilizing Eq.(53) and (54), the restriction on the DM mass

$$\frac{m_j}{\text{GeV}} \geq \frac{6.1 \times 10^{-7}}{\tilde{\mu}_1 \beta^{1/4}} \left(\frac{m_{\text{WDM}}}{\text{keV}} \right)^{4/3} \left(\frac{M_{\text{in}}}{M_P} \right)^{\frac{1-w_\phi}{2(1+w_\phi)}}, \quad (55)$$

For example, if one takes 10 g of initial PBH, the DM mass bound turns out to be $m_j > \frac{5.1 \times 10^{-5}}{\beta^{1/4}}$ GeV, for $w_\phi = 1/2$. Now let us move our discussion to the case of inflation reheating.

4. $\beta < \beta_c$ (Inflaton reheating)

If the coupling strength $y_\phi > y_\phi^c$ and $\beta < \beta_c$, inflaton coupling determines reheating temperature. In addition to that depending on how strong the coupling is $y_\phi > y_\phi^{\text{th}}$ or $y_\phi^c < y_\phi < y_\phi^{\text{th}}$, reheating happen before and after the evaporation point, respectively. The restriction would be different in these two cases.

- $a_{\text{ev}} < a_{\text{RH}}$: Once $y_\phi^c < y_\phi < y_\phi^{\text{th}}$, reheating occurs after completion of the evaporation process. One can find the ratio $a_{\text{ev}}/a_{\text{eq}}$ as

$$\frac{a_{\text{ev}}}{a_{\text{eq}}} = \frac{a_{\text{ev}}}{a_{\text{RH}}} \frac{a_{\text{RH}}}{a_{\text{eq}}} = \left(\frac{g_{\text{eq}}^s}{g_{\text{RH}}^s} \right)^{1/3} \frac{T_{\text{eq}}}{T_{\text{RH}}} \tilde{\mu}_2 \left(\frac{T_{\text{RH}}^2}{M_P^2} \frac{M_{\text{in}}^3}{M_P^3} \right)^{\frac{2}{3(1+w_\phi)}}, \quad (56)$$

where $\tilde{\mu}_2 = \left(\frac{1+w_\phi}{2\epsilon} \sqrt{\frac{\alpha_T}{3}} \right)^{\frac{2}{3(1+w_\phi)}}$. To derive above equation we use Eq.(33). Now, upon substitution of the above Eq.(56) into (50) and employing Eq.(51), we get

$$\frac{m_j}{\text{GeV}} \geq 1.2 \times 10^{-6} \tilde{\mu}_2 \left(\frac{m_{\text{WDM}}}{\text{keV}} \right)^{4/3} \left(\frac{T_{\text{RH}}}{M_P} \right)^{\frac{1-3w_\phi}{3(1+w_\phi)}} \left(\frac{M_{\text{in}}}{M_P} \right)^{\frac{1-w_\phi}{1+w_\phi}}. \quad (57)$$

For example, if one takes 10 g of initial PBH mass, the DM mass bound turns out to be $m_j > \left(\frac{T_{\text{RH}}}{\text{GeV}} \right)^{-1/9} 6.6 \times 10^{-2}$ GeV, for $w_\phi = 1/2$.

- $a_{\text{ev}} > a_{\text{RH}}$: For strong coupling $y_\phi > y_\phi^{\text{th}} > y_\phi^c$, the reheating process completes even before the evaporation point, and the leading decay process takes

place in a radiation-dominated background. In this case, $T(a_{\text{ev}})$ can be calculated from the Hubble parameter at the evaporation point, which is related to Γ_{BH} , $H(a_{\text{ev}}) = \frac{\Gamma_{\text{BH}}}{2} = \frac{3\epsilon}{2} \frac{M_P^4}{M_{\text{in}}^3}$. The evaporation temperature

$$T(a_{\text{ev}}) = \left(\frac{3 M_P^2 H(a_{\text{ev}})^2}{\alpha_T} \right)^{\frac{1}{4}} = \left(\frac{27 \epsilon^2}{4 \alpha_T} \right)^{\frac{1}{4}} \frac{M_P^{\frac{3}{2}}}{M_{\text{in}}^{\frac{3}{2}}}. \quad (58)$$

Since in this scenario, after evaporation no entropy injection in the Universe, combining Eq.(53) and (58), one can find

$$\frac{m_j}{\text{GeV}} \geq 8.1 \times 10^{-7} \left(\frac{m_{\text{WDM}}}{\text{keV}} \right)^{\frac{4}{3}} \left(\frac{M_{\text{in}}}{M_P} \right)^{\frac{1}{2}}. \quad (59)$$

This particular constraint is similar to the one previously discussed for the PBH-dominated case (see Eq.(52)). This behavior was expected because it corresponds to our naive estimate of the boost factor γ discussed previously.

We depicted in Fig.(7) how DM parameter space presented in Fig.(5) is modified if one considers WDM constraints, which we show in orange shaded region. One important outcome of Fig.(7) is that for $m_j < T_{\text{BH}}^{\text{in}}$, the allowed DM masses in the context of purely PBH reheating is severely restricted due to the violation of the WDM limit.

C. PBH evaporation: Comparison with the exact greybody factor

PBH mass reduction rate is crucially dependent on evaporation process, produced particles' spin, and the angular momentum of the BHs [34]. Throughout our analysis we dealt with the Schwarzschild BHs, To be precise the rate of change of BH mass is calculated upon integrating over the phase space and summing over different species as

$$\frac{dM_{\text{BH}}}{dt} = - \sum_j \int_0^\infty E_j \frac{\partial^2 N_j}{\partial p \partial t} dp = -\epsilon(M_{\text{BH}}) \frac{M_P^4}{M_{\text{BH}}^2}, \quad (60)$$

where $\frac{\partial^2 N_j}{\partial p \partial t}$ represents the emission rate of any species j of mass m_j and spin s_j with degrees of freedom g_j in time interval dt and momentum lies within⁵ $(p, p + dp)$ and $E_j = \sqrt{m_j^2 + p^2}$. The BH mass-dependent evaporation function $\epsilon(M_{\text{BH}})$ can be expressed as

$$\epsilon(M_{\text{BH}}) = \sum_j g_j \epsilon_j(z_j), \quad (61)$$

where

$$\epsilon_j(z_j) = \frac{27}{128 \pi^3} \int_0^\infty \frac{\Psi_{s_j} (x_j^2 - z_j^2)}{\exp(x_j) - (-1)^{2s_j}} x_j dx_j, \quad (62)$$

where x_j and z_j are the dimensionless parameter defined as $x_j = E_j/T_{\text{BH}}$, $z_j = m_j/T_{\text{BH}}$. And Ψ_{s_j} is the reduced greybody factor defined as the ratio between the exact greybody factor to its value in the *geometrical-optics* limit

$$\Psi_{s_j}(x) = \frac{\sigma_{s_j}}{\sigma_{s_j}|_{\text{go}}}. \quad (63)$$

In the *geometrical-optics* limit, the greybody factor assumes, $\sigma_{s_j}|_{\text{go}} = \frac{27}{64\pi} \frac{M_{\text{BH}}^2}{M_P^4}$ [60–63] and the evaporation function for massless particle turns out as

$$\epsilon_j(0) = \frac{27 \xi \pi g_j}{4 \cdot 480}, \quad (64)$$

where $\xi = (1, 7/8)$ for bosons and fermions respectively, which is the limit we took. Consequently, PBH mass evolution follows Eq.(2).

One important point to note is that the evaporation function in the *geometrical-optics* limit nearly matches with the actual evaporation function for scalar and fermionic particles, however for fermion mass $m_j > 4T_{\text{BH}}$ our calculation is slightly underestimated compare to the actual one, as we can see from the Fig.(2) of Ref.[34] where they plotted the evaporation function $\epsilon_j(z_j)$ as function of z_j . Finally, we can add that for scalar (spin zero) and fermionic (spin half) particles, the *geometrical-optical* limit works fine, whereas for higher spin particles such as spin-1 and spin-2 particles, we would need to take the exact spectrum for the accurate analysis.

IV. CONCLUSION

In this study, we have compared in detail the DM parameter space in the background of the reheating phase dynamically obtained from two chief systems in the early Universe: the inflaton ϕ and the primordial black holes. The DM is assumed to be produced purely gravitationally from the PBH decay, not interacting with the thermal bath and the inflaton. Within this context, The population of the primordial black holes behaves like dust, whereas the behavior of inflaton depends strongly on its equation of state after the inflationary phase, which in turn depends on the exponent of the potential $V(\phi) \propto \phi^n$, $w_\phi = \frac{n-2}{n+2}$. Depending upon the dynamics of reheating, we showed that a large range of initial PBH masses M_{in} and fraction β can lead to the right amount of relic abundance.

If PBHs dominate the background dynamics ($\beta > \beta_c$), the reheating process becomes insensitive to the inflaton and the PBH fraction β . Therefore, it is the PBH

⁵ For details calculation, see Ref.[34].

mass M_{in} that solely controls the DM abundance as well as the reheating temperature T_{RH} . In this scenario, if $m_j < T_{\text{BH}}^{\text{in}}$, with increasing DM mass, we need to increase the value of M_{in} to increase the dilution such that the DM number density decreases to avoid the DM overproduction i.e., $m_j \propto \sqrt{M_{\text{in}}}$. Another possibility is to have DM mass $m_j > T_{\text{BH}}^{\text{in}}$, where the Boltzmann suppression naturally reduces the DM production and hence opens up the lower M_{in} values for which abundance could be satisfied. This scenario is nicely illustrated by Fig.(1).

If one considers $y_\phi < y_\phi^c$ and $\beta < \beta_c$ that allows PBH radiation to govern the reheating while the inflaton dominates the energy budget during the whole process. For such case, the allowed DM region can be extended, and that is solely dependent on the inflaton equation of state w_ϕ . As an example we have shown the results for $w_\phi = 1/2$ in Fig.(2). The main conclusion of our analysis is that two very secluded region of PBH parameters can, at the same time ensures a successful reheating while still producing the right amount of dark matter with mass m_j : 10^{-4} GeV $\lesssim m_j \lesssim 1$ GeV (corresponding to $m_j \ll T_{\text{BH}}^{\text{in}}$), and 10^{19} GeV $\gtrsim m_j \gtrsim 10^8$ GeV (corresponding to $m_j \gg T_{\text{BH}}^{\text{in}}$).

In the case of extended mass function with power-law distribution extending to lower PBH mass values, the limits in the lower DM regime ($m_j < T_{\text{BH}}^{\text{in}}$) remain unchanged compared to the monochromatic scenario. However, in the high DM mass regime ($m_j > T_{\text{BH}}^{\text{in}}$) gets modified depending on the width of the distribution. For instance, with $\sigma = 2$, the constraint on the range of allowed values for m_j becomes 10^{19} GeV $\gtrsim m_j \gtrsim 10^{12}$ GeV.

If the energy budget *and* the reheating is dominated by the inflaton, the range of allowed DM mass is widened and depends strongly on the Yukawa coupling of the inflaton to the Standard Model, y_ϕ as one can see in Fig.(5) which can be considered as the master plot of our work. In comparison with the PBH reheating, a noticeable difference in DM parameter space can be observed in both $m_j < T_{\text{BH}}^{\text{in}}$ and $m_j > T_{\text{BH}}^{\text{in}}$ case. Particularly when $m_j > T_{\text{BH}}^{\text{in}}$, for which DM yield is large for lower PBH and DM mass, $\Omega_j h^2 \propto M_{\text{in}}^{-5/3} m_j^{-1}$ compare to PBH reheating $\Omega_j h^2 \propto M_{\text{in}}^{-13/6} m_j^{-1}$ for $w_\phi = 1/2$. In this case, additional entropy injection from inflaton dilutes the yields. Consequently, it allows lower PBH masses to not overclose the Universe. Hence, the increment of the inflaton coupling y_ϕ widen the mass range by rendering both lower values of m_j and M_{in} viable for $y_\phi \sim 0.05$ as we see in Fig.(5). Interestingly for $m_j < T_{\text{BH}}^{\text{in}}$ case, on the other hand, the dilution due to entropy injection effects oppositely on the DM yields, $\Omega_j h^2 \propto M_{\text{in}}^{1/3} m_j$ for $w_\phi = 1/2$, rendering it under abundant. Thus, one must increase the m_j value in inflation reheating to obtain the correct DM yield with increasing y_ϕ . Indeed, the decoupling between the reheating process (completed by the inflaton) and the dark matter production (generated by the PBHs) allows for a larger range of dilution factor

through the injection of the entropy from inflaton decay. As a consequence, larger DM mass are necessary for the same amount of relic abundance. Moreover, in PBH reheating, for $m_j < T_{\text{BH}}^{\text{in}}$, $m_j \propto M_{\text{in}}^{1/6}$, whereas inflation reheating suggests $m_j \propto M_{\text{in}}^{-1/3}$, which is a completely opposite behavior which we can see in Fig.(5).

We have also included the warm dark matter constraints from structure formation and Lyman- α forest. Indeed, the dark matter momentum at evaporation time being $p_{\text{ev}} \sim T_{\text{BH}}^{\text{in}} \gg T_{\text{RH}}$, the typical limit $m_j \gtrsim 3$ keV needs to be revisited. We considered this boost factor in our analysis, which makes the dark matter candidate relativistic for longer. We found that the region $m_j < T_{\text{BH}}^{\text{in}}$ previously allowed for pure PBH reheating is now excluded due to warm dark matter limit, whereas the region $m_j > T_{\text{BH}}^{\text{in}}$ stays unaffected as we can see in Fig.(7). On the other hand, the presence of the inflaton produces a sufficiently large amount of entropy, decreasing the free streaming length significantly. In this case, the warm dark matter constraint does not affect our result either, as we also see in Fig.(7).

In conclusion, we see that the combination of two chief systems of the world, even with very different phenomenology and dynamics, can considerably enlarge the parameter space allowed by the cross-constraints from reheating and the relic abundance.

ACKNOWLEDGMENTS

E.K. and Y.M. want to thank L. Heurtier for extremely valuable discussions during the completion of our work. This project has received support from the European Union's Horizon 2020 research and innovation programme under the Marie Skłodowska-Curie grant agreement No 860881-HIDDeN, and the IN2P3 Master Projet UCMN. M.R.H wishes to acknowledge support from the Science and Engineering Research Board (SERB), Government of India (GoI), for the SERB National Post-Doctoral fellowship, File Number: PDF/2022/002988. DM wishes to acknowledge support from the Science and Engineering Research Board (SERB), Department of Science and Technology (DST), Government of India (GoI), through the Core Research Grant CRG/2020/003664. DM also thanks the Gravity and High Energy Physics groups at IIT Guwahati for illuminating discussions. The work of E.K. was supported by the grant "Margarita Salas" for the training of young doctors (CA1/RSUE/2021-00899), co-financed by the Ministry of Universities, the Recovery, Transformation and Resilience Plan, and the Autonomous University of Madrid.

Appendix A: Expression for the critical coupling y_ϕ^c

In the standard reheating scenario, the reheating process is not instantaneous, and during this phase, the inflaton energy density transfers to the daughter particles, mostly to the SM particles, setting proper initial conditions for the Big Bang Nucleosynthesis (BBN). In principle, considering different gravitational and non-gravitational couplings, there are several possibilities for reheating. However, in this analysis, we are only interested in the fermionic coupling with interaction Lagrangian $y_\phi \phi \bar{f} f$. Taking such a scenario, we have the radiation energy density

$$\rho_R^D(a) = \frac{y_\phi^2}{8\pi} \lambda^{\frac{1-w_\phi}{2(1+w_\phi)}} \alpha_n M_P^4 \left(\frac{\rho_{\text{end}}}{M_P^4} \right)^{\frac{3}{2} - \frac{1}{1+w_\phi}} \left(\frac{a}{a_{\text{end}}} \right)^{-4} \times \left[\left(\frac{a}{a_{\text{end}}} \right)^{\frac{5-9w_\phi}{2}} - 1 \right], \quad (\text{A1})$$

where a_{end} is the scale factor associated with the end of inflation, and λ is related to the mass scale Λ of the α -attractor potential [44, 45], $\lambda = \left(\frac{\Lambda}{M_P} \right)^4 \left(\frac{2}{3\alpha} \right)^{\frac{n}{2}}$, potential which has the form

$$V(\phi) = \Lambda^4 \left[1 - e^{-\sqrt{\frac{2}{3\alpha}} \frac{\phi}{M_P}} \right]^n. \quad (\text{A2})$$

The parameter λ can be represented in terms of the CMB observables, such as the amplitude of the inflaton fluctuation $A_{\mathcal{R}}$ and scalar spectral index n_s as [46]

$$\lambda = \left(\frac{2}{3\alpha} \right)^{\frac{n}{2}} \left(\frac{3\pi^2 r A_{\mathcal{R}}}{2} \right)^4 \times \left[\frac{n^2 + n + \sqrt{n^2 + 3\alpha(2+n)(1-n_s)}}{n(2+n)} \right]^n \quad (\text{A3})$$

The above equation suggests that the evolution of the radiation energy density is different for $w_\phi > 5/9$ ($n > 7$) and $w_\phi < 5/9$ ($n < 7$). As a consequence, the end of the reheating, which is defined at the point of a_{RH} where $\rho_\phi(a_{\text{RH}}) = \rho_R(a_{\text{RH}}) = \rho_{\text{RH}}$ would be different for $n > 7$ and $n < 7$. In the case of $n < 7$, a_{RH} can be written as [13, 14],

$$\frac{a_{\text{RH}}}{a_{\text{end}}} = \left[\frac{y_\phi^2}{8\pi} \alpha_n \left(\frac{\lambda M_P^4}{\rho_{\text{end}}} \right)^{\frac{1-w_\phi}{2(1+w_\phi)}} \right]^{\frac{2}{3(w_\phi-1)}}. \quad (\text{A4})$$

However for $n > 7$ one can find

$$\frac{a_{\text{RH}}}{a_{\text{end}}} = \left[-\frac{y_\phi^2}{8\pi} \alpha_n \left(\frac{\lambda M_P^4}{\rho_{\text{end}}} \right)^{\frac{1-w_\phi}{2(1+w_\phi)}} \right]^{\frac{1}{1-3w_\phi}}. \quad (\text{A5})$$

Upon substitution, the expression for a_{RH} Eq.(A5) and (A5) into (A1) ρ_{RH} can be written as,

$$\rho_{\text{RH}}^D = \left(\frac{y_\phi^2}{8\pi} \alpha_n \right)^{\frac{2(1+w_\phi)}{1-w_\phi}} \lambda M_P^4. \quad (\text{A6})$$

Whereas, for $n > 7$,

$$\rho_{\text{RH}}^D = \left(\frac{y_\phi^2}{8\pi} \alpha_n \right)^{\frac{3(1+w_\phi)}{3w_\phi-1}} (\lambda M_P^4)^{\frac{3(1-w_\phi)}{2(3w_\phi-1)}} \rho_{\text{end}}^{\frac{5-9w_\phi}{2(1-3w_\phi)}}. \quad (\text{A7})$$

The expression for the critical coupling y_ϕ^c below which value PBH-driven reheating happens should be followed

$$\rho_{\text{RH}} = \rho_{\text{RH}}^D, \quad (\text{A8})$$

where the left-hand side calculated only taking PBH evaporation as a source and the right-hand side for the inflaton decay. The radiation energy density at the end of PBH-driven reheating can be written as

$$\rho_{\text{RH}} = \rho_R(a_{\text{ev}}) \left(\frac{a_{\text{ev}}}{a_{\text{RH}}} \right)^4 \simeq \rho_{\text{BH}}(a_{\text{ev}}) \left(\frac{a_{\text{ev}}}{a_{\text{RH}}} \right)^4, \quad (\text{A9})$$

and the inflaton energy density

$$\rho_\phi(a_{\text{RH}}) = \rho_\phi(a_{\text{in}}) \left(\frac{a_{\text{in}}}{a_{\text{RH}}} \right)^{3(1+w_\phi)}. \quad (\text{A10})$$

Now upon substitution of Eq.(12) into Eq.(A9) and comparing with (A10), one can find

$$\left(\frac{a_{\text{ev}}}{a_{\text{RH}}} \right)^4 = \beta^{\frac{4}{3w_\phi-1}} \left(\frac{a_{\text{in}}}{a_{\text{ev}}} \right)^{\frac{12w_\phi}{1-3w_\phi}}. \quad (\text{A11})$$

Utilizing the above equation, ρ_{RH} can be written as,

$$\rho_{\text{RH}} = 48\pi^2 \beta^{\frac{3(1+w_\phi)}{3w_\phi-1}} \left(\frac{\epsilon}{2(1+w_\phi)\pi\gamma^{3w_\phi}} \right)^{\frac{2}{1-3w_\phi}} \left(\frac{M_P}{M_{\text{in}}} \right)^{\frac{6(1-w_\phi)}{1-3w_\phi}} M_P^4. \quad (\text{A12})$$

Connecting Equations (A12), (A8) and (A6), we have

$$y_\phi^c = \sqrt{\frac{8\pi}{\alpha_n}} \beta^{\frac{3(1-w_\phi)}{4(3w_\phi-1)}} \left(\frac{48\pi^2}{\lambda} \right)^{\frac{1-w_\phi}{4(1+w_\phi)}} \left(\frac{\epsilon \gamma^{-3w_\phi}}{2\pi(1+w_\phi)} \right)^{\frac{1-w_\phi}{2(1-3w_\phi)(1+w_\phi)}} \left(\frac{M_P}{M_{\text{in}}} \right)^{\frac{3}{2} \frac{(1-w_\phi)^2}{(1-3w_\phi)(1+w_\phi)}}, \quad (\text{A13})$$

where $\alpha_n = \frac{2(1+w_\phi)}{(5-9w_\phi)} \sqrt{\frac{6(1+w_\phi)(1+3w_\phi)}{(1-w_\phi)^2}}$. The above equation is true for $n < 7$. For $n > 7$, similarly, instead of

using Eq.(A6) employing Eq.(A7), one can find

$$y_\phi^c = \sqrt{-\frac{8\pi\beta}{\alpha_n}} (48\pi^2)^{\frac{3w_\phi-1}{6(1+w_\phi)}} \lambda^{\frac{w_\phi-1}{4(1+w_\phi)}} \left(\frac{\epsilon\gamma^{-3w_\phi}}{2\pi(1+w_\phi)}\right)^{-\frac{1}{3(1+w_\phi)}} \left(\frac{M_P}{M_{\text{in}}}\right)^{\frac{1-w_\phi}{1+w_\phi}} \left(\frac{\rho_{\text{end}}}{M_P^4}\right)^{\frac{5-9w_\phi}{12(1+w_\phi)}} \quad (\text{A14})$$

Appendix B: Expression for y_ϕ^{th}

The coupling strength y_ϕ^{th} which ensures that the inflaton reheating happens before the evaporation process completes, can be determined by equating $a_{\text{ev}} \sim a_{\text{RH}}$, where expression for $a_{\text{RH}}/a_{\text{end}}$ is followed by Eq.(A4) for $n < 7$ and Eq.(A5) for $n > 7$. And $a_{\text{ev}}/a_{\text{end}}$ followed by the expression (see, for instance, Ref.[16])

$$\frac{a_{\text{ev}}}{a_{\text{end}}} = \left[\frac{(1+w_\phi)}{2\sqrt{3}\epsilon} \frac{M_{\text{in}}^3 \sqrt{\rho_{\text{end}}}}{M_P^5} \right]^{\frac{2}{3(1+w_\phi)}} \quad (\text{B1})$$

Now, comparing the above equations, for $n < 7$, we have

$$y_\phi^{\text{th}} = \nu_1 \left(\frac{M_P}{M_{\text{in}}} \right)^{\frac{3(1-w_\phi)}{2(1+w_\phi)}}, \quad (\text{B2})$$

and for $n > 7$

$$y_\phi^{\text{th}} = \nu_2 \left(\frac{M_{\text{in}}}{M_P} \right)^{\frac{1-3w_\phi}{1+w_\phi}} \left(\frac{\rho_{\text{end}}}{M_P^4} \right)^{\frac{5-9w_\phi}{12(1+w_\phi)}}, \quad (\text{B3})$$

$$\text{where } \nu_1 = \sqrt{\frac{8\pi}{\alpha_n}} \left(\frac{1+w_\phi}{2\epsilon} \sqrt{\frac{\lambda}{3}} \right)^{\frac{w_\phi-1}{2(1+w_\phi)}} \text{ and } \nu_2 = \sqrt{-\frac{8\pi}{\alpha_n}} \left(\frac{1+w_\phi}{2\sqrt{3}\epsilon} \right)^{\frac{1-3w_\phi}{3(1+w_\phi)}} \lambda^{\frac{w_\phi-1}{4(1+w_\phi)}}.$$

-
- [1] S. W. Hawking, Nature **248**, 30-31 (1974)
- [2] S. W. Hawking, Commun. Math. Phys. **43**, 199-220 (1975) [erratum: Commun. Math. Phys. **46**, 206 (1976)]
- [3] K. A. Olive, Phys. Rept. **190**, 307-403 (1990)
- [4] D. H. Lyth and A. Riotto, Phys. Rept. **314**, 1-146 (1999) [[arXiv:hep-ph/9807278](#) [hep-ph]].
- [5] J. Martin, C. Ringeval and V. Vennin, Phys. Dark Univ. **5-6**, 75-235 (2014) [[arXiv:1303.3787](#) [astro-ph.CO]].
- [6] J. Martin, C. Ringeval, R. Trotta and V. Vennin, JCAP **03**, 039 (2014) [[arXiv:1312.3529](#) [astro-ph.CO]].
- [7] J. Martin, Astrophys. Space Sci. Proc. **45**, 41 (2016) [[arXiv:1502.05733](#) [astro-ph.CO]].
- [8] Y. Mambrini, Particles in the dark Universe, *Springer Ed., ISBN 978-3-030-78139-2 (2021)*.
- [9] A. D. Dolgov and A. D. Linde, Phys. Lett. B **116** (1982), 329.
- [10] L. Kofman, A. D. Linde and A. A. Starobinsky, Phys. Rev. D **56** (1997), 3258-3295 [[arXiv:hep-ph/9704452](#) [hep-ph]].
- [11] M. A. G. Garcia, K. Kaneta, Y. Mambrini, K. A. Olive and S. Verner, JCAP **03** (2022) no.03, 016 [[arXiv:2109.13280](#) [hep-ph]].
- [12] O. Lebedev, Y. Mambrini and J. H. Yoon, [[arXiv:2305.05682](#) [hep-ph]].
- [13] M. A. G. Garcia, K. Kaneta, Y. Mambrini and K. A. Olive, JCAP **04** (2021), 012 [[arXiv:2012.10756](#) [hep-ph]].
- [14] M. A. G. Garcia, K. Kaneta, Y. Mambrini and K. A. Olive, Phys. Rev. D **101** (2020) no.12, 123507 [[arXiv:2004.08404](#) [hep-ph]].
- [15] M. R. Haque, D. Maity and P. Saha, Phys. Rev. D **102** (2020) no.8, 083534 [[arXiv:2009.02794](#) [hep-th]].
- [16] M. Riajul Haque, E. Kpatcha, D. Maity and Y. Mambrini, [[arXiv:2305.10518](#) [hep-ph]].
- [17] M. R. Haque, D. Maity, T. Paul and L. Sriramkumar, Phys. Rev. D **104**, no.6, 063513 (2021) [[arXiv:2105.09242](#) [astro-ph.CO]].
- [18] A. Chakraborty, M. R. Haque, D. Maity and R. Mondal, Phys. Rev. D **108**, no.2, 023515 (2023) [[arXiv:2304.13637](#) [astro-ph.CO]].
- [19] F. Zwicky, Helv. Phys. Acta **6** (1933), 110-127 doi:10.1007/s10714-008-0707-4
- [20] G. Arcadi, M. Dutra, P. Ghosh, M. Lindner, Y. Mambrini, M. Pierre, S. Profumo and F. S. Queiroz, Eur. Phys. J. C **78** (2018) no.3, 203 [[arXiv:1703.07364](#) [hep-ph]].
- [21] MD R. Haque and D. Maity, and R. Mondal, arXiv: 2301.01641.
- [22] N. Bernal, M. Heikinheimo, T. Tenkanen, K. Tuominen and V. Vaskonen, Int. J. Mod. Phys. A **32** (2017) no.27, 1730023 [[arXiv:1706.07442](#) [hep-ph]].
- [23] D. Chowdhury, E. Dudas, M. Dutra and Y. Mambrini, Phys. Rev. D **99** (2019) no.9, 095028 [[arXiv:1811.01947](#) [hep-ph]].
- [24] G. Bhattacharyya, M. Dutra, Y. Mambrini and M. Pierre, Phys. Rev. D **98** (2018) no.3, 035038 [[arXiv:1806.00016](#) [hep-ph]].
- [25] Y. Mambrini and K. A. Olive, Phys. Rev. D **103** (2021) no.11, 115009 [[arXiv:2102.06214](#) [hep-ph]].
- [26] M. R. Haque and D. Maity, Phys. Rev. D **107** (2023) no.4, 043531 [[arXiv:2201.02348](#) [hep-ph]].
- [27] S. Clery, Y. Mambrini, K. A. Olive, A. Shkerin and S. Verner, Phys. Rev. D **105** (2022) no.9, 095042 [[arXiv:2203.02004](#) [hep-ph]].
- [28] M. R. Haque and D. Maity, Phys. Rev. D **106** (2022) no.2, 023506 [[arXiv:2112.14668](#) [hep-ph]].
- [29] R. Calabrese, M. Chianese, J. Gunn, G. Miele, S. Morisi and N. Saviano, Phys. Rev. D **107** (2023) no.12, 123537 [[arXiv:2305.13369](#) [hep-ph]].

- [30] I. Baldes, Q. Decant, D. C. Hooper and L. Lopez-Honorez, *JCAP* **08** (2020), 045 [[arXiv:2004.14773](#) [astro-ph.CO]].
- [31] N. Bernal and Ó. Zapata, *JCAP* **03** (2021), 007 [[arXiv:2010.09725](#) [hep-ph]].
- [32] A. Cheek, L. Heurtier, Y. F. Perez-Gonzalez and J. Turner, *Phys. Rev. D* **108** (2023) no.1, 015005 [[arXiv:2212.03878](#) [hep-ph]].
- [33] A. Cheek, L. Heurtier, Y. F. Perez-Gonzalez and J. Turner, *Phys. Rev. D* **106** (2022) no.10, 103012 [[arXiv:2207.09462](#) [astro-ph.CO]].
- [34] A. Cheek, L. Heurtier, Y. F. Perez-Gonzalez and J. Turner, *Phys. Rev. D* **105** (2022) no.1, 015022 [[arXiv:2107.00013](#) [hep-ph]].
- [35] I. Masina, *Eur. Phys. J. Plus* **135** (2020) no.7, 552 [[arXiv:2004.04740](#) [hep-ph]].
- [36] A. M. Green and B. J. Kavanagh, *J. Phys. G* **48** (2021) no.4, 043001 [[arXiv:2007.10722](#) [astro-ph.CO]].
- [37] B. J. Carr, *Lect. Notes Phys.* **631** (2003), 301-321 [[arXiv:astro-ph/0310838](#) [astro-ph]].
- [38] B. J. Carr and S. W. Hawking, *Mon. Not. Roy. Astron. Soc.* **168** (1974), 399-415
- [39] N. Aghanim *et al.* [Planck], *Astron. Astrophys.* **641**, A6 (2020) [[arXiv:1807.06209](#) [astro-ph.CO]].
- [40] P. Bode, J. P. Ostriker and N. Turok, *Astrophys. J.* **556**, 93-107 (2001) [[arXiv:astro-ph/0010389](#) [astro-ph]].
- [41] V. Iršič, M. Viel, M. G. Haehnelt, J. S. Bolton, S. Cristiani, G. Cupani, T. S. Kim, V. D'Odorico, S. López and S. Ellison, *et al.* *Phys. Rev. D* **96**, no.2, 023522 (2017) [[arXiv:1702.01764](#) [astro-ph.CO]].
- [42] M. Viel, G. D. Becker, J. S. Bolton and M. G. Haehnelt, *Phys. Rev. D* **88**, 043502 (2013) [[arXiv:1306.2314](#) [astro-ph.CO]].
- [43] S. Hoof, A. Geringer-Sameth and R. Trotta, *JCAP* **02**, 012 (2020) [[arXiv:1812.06986](#) [astro-ph.CO]].
- [44] J. Ellis, D. V. Nanopoulos and K. A. Olive, *JCAP* **10**, 009 (2013) [[arXiv:1307.3537](#) [hep-th]].
- [45] R. Kallosh, A. Linde and D. Roest, *JHEP* **11**, 198 (2013) [[arXiv:1311.0472](#) [hep-th]].
- [46] M. Drewes, J. U. Kang and U. R. Mun, *JHEP* **11**, 072 (2017) [[arXiv:1708.01197](#) [astro-ph.CO]].
- [47] B. Carr, M. Raidal, T. Tenkanen, V. Vaskonen and H. Veermäe, *Phys. Rev. D* **96** (2017) no.2, 023514 doi:10.1103/PhysRevD.96.023514 [[arXiv:1705.05567](#) [astro-ph.CO]].
- [48] B. J. Carr, *Astrophys. J.* **201** (1975), 1-19 doi:10.1086/153853
- [49] A. Dolgov and J. Silk, *Phys. Rev. D* **47** (1993), 4244-4255
- [50] A. M. Green, *Phys. Rev. D* **94** (2016) no.6, 063530 [[arXiv:1609.01143](#) [astro-ph.CO]].
- [51] A. D. Dolgov, M. Kawasaki and N. Kevlishvili, *Nucl. Phys. B* **807** (2009), 229-250 [[arXiv:0806.2986](#) [hep-ph]].
- [52] B. J. Carr, K. Kohri, Y. Sendouda and J. Yokoyama, *Phys. Rev. D* **94** (2016) no.4, 044029 [[arXiv:1604.05349](#) [astro-ph.CO]].
- [53] I. Musco and J. C. Miller, *Class. Quant. Grav.* **30** (2013), 145009 [[arXiv:1201.2379](#) [gr-qc]].
- [54] J. C. Niemeyer and K. Jedamzik, *Phys. Rev. D* **59** (1999), 124013 [[arXiv:astro-ph/9901292](#) [astro-ph]].
- [55] J. Yokoyama, *Phys. Rev. D* **58** (1998), 107502 [[arXiv:gr-qc/9804041](#) [gr-qc]].
- [56] J. Martin, T. Papanikolaou and V. Vennin, *JCAP* **01** (2020), 024 [[arXiv:1907.04236](#) [astro-ph.CO]].
- [57] J. Martin, T. Papanikolaou, L. Pinol and V. Vennin, *JCAP* **05** (2020), 003 [[arXiv:2002.01820](#) [astro-ph.CO]].
- [58] P. Auclair and V. Vennin, *JCAP* **02** (2021), 038 [[arXiv:2011.05633](#) [astro-ph.CO]].
- [59] A. Cheek, L. Heurtier, Y. F. Perez-Gonzalez and J. Turner, *Phys. Rev. D* **105** (2022) no.1, 015023 [[arXiv:2107.00016](#) [hep-ph]].
- [60] D. N. Page, *Phys. Rev. D* **13**, 198-206 (1976)
- [61] D. N. Page, *Phys. Rev. D* **16**, 2402-2411 (1977)
- [62] J. H. MacGibbon and B. R. Webber, *Phys. Rev. D* **41**, 3052-3079 (1990)
- [63] J. H. MacGibbon, *Phys. Rev. D* **44**, 376-392 (1991)